## ABSTRACT

## CHEMICAL VAPOR DEPOSITION OF POLYMERIC CARBON FILMS

**by**

**Chi Yu**

Poly-peri-naphthalene (PPN) is a one-dimensional (1-D) graphite polymer with unique planar ladder-like conjugated molecular structure. PPN was predicted to be a good intrinsic conductor and have high thermal stability and high environmental stability.

In this project, chemical vapor deposition (CVD) and plasma enhanced chemical vapor deposition (PECVD) of carbon films with PPN structure using PTCDA as precursor were carried out under different conditions. There is only limited information in literature on the synthesis of PPN films by PECVD process, which may allow deposition at a higher rate with lower substrate temperature. In this work the influence of deposition parameters, such as sublimation temperature, substrate (pyrolysis) temperature, pressure, plasma condition on the structure of deposition product was systematically studied. It's found that the following deposition parameters are required for carbon films containing PPN structure:

1. CVD: sublimation temperature 510°C for PTCDA and substrate temperature around 380°C in atmosphere pressure. This confirms the results of previous studies of this material.

2. PECVD: sublimation temperature and substrate temperature both approximate 350°C, with DC discharge power of several watts, stable plasma in argon gas of approximate 1 torr pressure.

In the synthesis of PPN films by both methods, substrate temperature plays an important role that affects quality of the films.

# CHEMICAL VAPOR DEPOSITION OF POLYMERIC CARBON FILMS

by
Chi Yu

A Thesis
Submitted to the Faculty of
New Jersey Institute of Technology
In Partial Fulfillment of the Requirements for the Degree of
Master of Science in Materials Science and Engineering

Interdisciplinary Program in Materials Science and Engineering

January 2004

**APPROVAL PAGE**

**CHEMICAL VAPOR DEPOSITION OF POLYMERIC CARBON FILMS**

**Chi Yu**

Dr. Marek Sosnowski, Thesis Advisor — Date
Professor of Electrical and Computer Engineering, NJIT

Dr. Haim Grebel, Committee Member — Date
Professor of Electrical and Computer Engineering, NJIT

Dr. Zafar Iqbal, Committee Member — Date
Research Professor of Chemistry, NJIT

## BIOGRAPHICAL SKETCH

**Author:** Chi Yu

**Degree:** Master of Science

**Undergraduate and Graduate Education:**

- Master of Science in Materials Science and Engineering
  New Jersey Institute of Technology, Newark, NJ, 2004
- M.S. Candidate in Materials Science
  Sichuan University, Chengdu, P.R. China, 2001
- Bachelor of Science in Materials Science
  Sichuan University, Chengdu, P.R. China, 1996

**Major:** Materials Science and Engineering

**Publications:**

Chi Yu, Jianguo Zhu, Ding-quan Xiao, Xiao-wu Yuang, Ji-liang Zhu, Xi Yeu (2001) "Preparation of Lanthanum Modified Bismuth Titanate Ferroelectric Thin Film by SOL-GEL Processing", Piezoelectrics & Acoustooptics, 23: 138-141.

Jianguo Zhu, Chi Yu, Ding-quan Xiao, Wen Zhang, Xiao-wu Yuang, Ji-liang Zhu, Xi Yeu (2001) "The Structural, Dielectric and Ferroelectric Properties of La-modified Bismuth Titanate Thin Films Prepared by SOL-GEL Process", 2001 IEEE Proceeding 0-7803-5940-2/01, 579-582.

To my dear husband

## ACKNOWLEDGEMENT

I would like to express my sincerest gratitude to Professor Marek Sosnowski, who served as my research advisor and provided great guidance throughout the whole research. I would like to express my appreciation to Professor Zafar Iqbal and Professor Haim Grebel for helping in Raman spectral test and serving as members of the thesis committee.

Sincere thanks to Dr. Leszek Gladczuk for his generous help and valuable suggestions during the progress of the work.

I had the pleasure of working with Ms. Wenwen Lou, Mr. Amid Goyal, Dr. Yan Zhang, Dr. Xueyan Zhang, Ms. Jing Chen and Yishay S Diamant, their help are appreciated.

Finally, I want to thank my dear husband, parents and sister for their support and encouragement.

## TABLE OF CONTENTS

**TABLE OF CONTENTS**
**(Continued)**

**Chapter** **Page**

## TABLE OF CONTENTS
## (Continued)

## LIST OF TABLES

## LIST OF FIGURES

## LIST OF FIGURES
## (Continued)

# CHAPTER 1

# INTRODUCTION

## 1.1 Introduction to Polymeric Carbon Films

### 1.1.1 Carbon and Carbon Films

The field of disordered carbon covers a wide range of materials and properties which includes chars of organic materials, carbon black, soot, polymeric carbon, diamond-like carbon, *etc.* [1]

With different orbital hybridization: sp, $sp^2$, $sp^3$, carbon have different structure: carbyne, graphite, fullerene and diamond, as shown in Figure 1.1. Another form of carbon, nanotube, has mixed $sp^2$-$sp^3$ hybridization.

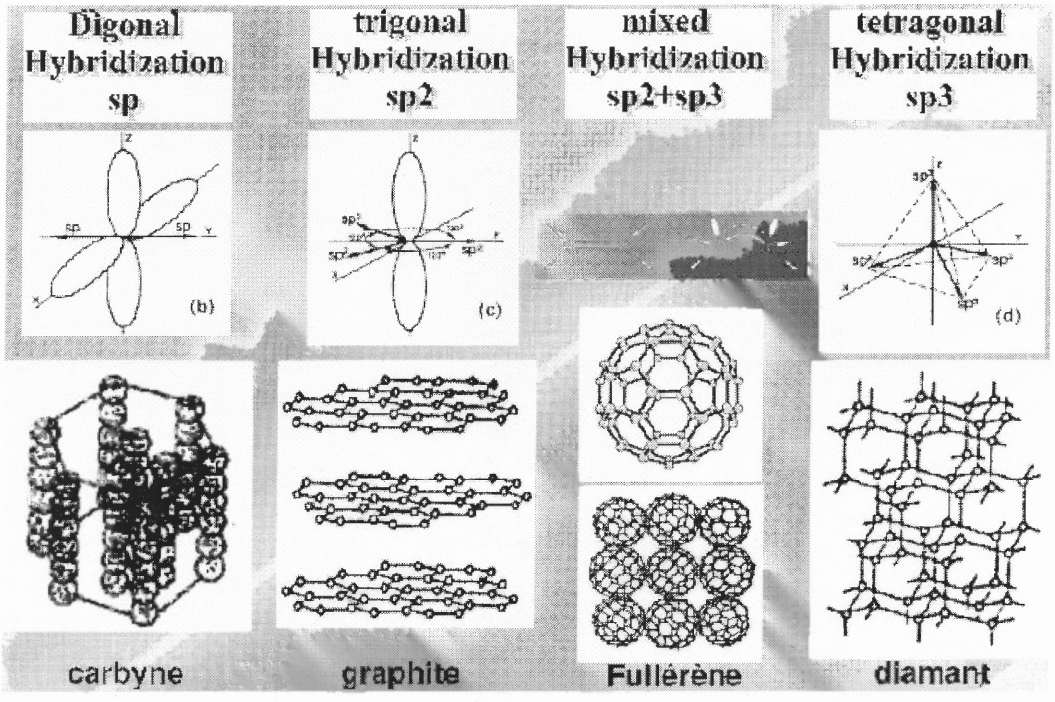


Figure 1.1 Structures of carbon. [2]

Carbon films are distinguished by their broad structural variability: graphitic (trigonal) or diamond-like (tetrahedral) bonds, crystalline or amorphous atomic arrangements, homogeneous films or lamellar/globular/cylindrical heterostructures [3].

Carbon films have been prepared by many methods: pyrolysis and the consequent carbonization of an initial organic phase, laser induced vacuum deposition (Laser-Arc), pulsed laser deposition, ion beam deposition, reactive magnetron sputtering, electron beam evaporation of carbon, organic molecular beam deposition, chemical vapor deposition (CVD) and plasma enhanced chemical vapor deposition (PECVD) etc.

The numerous applications of carbon films are related to their particular characteristics: light weight associated with a high mechanical strength, including stiffness, wear, toughness and thermal shock resistance [4]. An example is dielectric films of amorphous hydrogenated diamond-like carbon (a-C:H DLC or DLC); they have been shown to have high hardness, low friction, electrical insulation, chemical inertness, biological compatibility, ability to absorb photons selectively, smoothness, resistance to wear, and other interesting electrical and optical properties.

### 1.1.2 Polymeric Carbon Films

"Polymeric carbon" is a generic term embracing all carbons produced directly by the carbonization of polymers without passing through a plastic coking phase, the old classification being that of "char." The terminology relates to glassy carbon, charcoal, and carbon fibers. These have been shown to embody a network of microfibrils

consisting of stacked graphitic ribbons. [5]

Polymeric carbon thin films offer attractive features such as low density, high strength, stiffness, dimensional stability, low dielectric constant, resistance to extreme environmental effects, and their ability to be metallized or coated.

## 1.2 Chemical Vapor Deposition (CVD) Method for Carbon Films

Chemical Vapor Deposition (CVD) and plasma-enhanced chemical vapor deposition (PECVD) technique are the most common and the most effective methods for the deposition of thin films, that can be also applied to carbon.

### 1.2.1 CVD

Deposited species are formed as a result of chemical reaction between gaseous reactants in an inert gas at elevated temperature in the vicinity of the substrate; solid product of the reaction is deposited on the surface of the hot substrate surface.

CVD is based on competition between chemical reactions and physical transport. The process is driven by thermal energy.

### 1.2.2 PECVD

Plasma Enhanced Chemical Vapor Deposition (PECVD) is a modification of chemical vapor deposition in which chemical reactions between gaseous species resulting in deposition of a solid are activated by electrical gas discharge (plasma).

Advantages of PECVD include: lower operating temperature; higher deposition

rate, wide range of products and the control of film properties, more efficient precursors and energy utilization with less waste product generation , applicability to deposition on large-area substrates, very uniform coatings, and suitability to very large-scale production. PECVD starting from organic compounds is effective in the preparation of thin solid films with a dense and pin-hole-free structure suitable for materials used in making up electrically insulating layers, protective surface coatings, etc [6].

**Free Radicals**

When an electric field is introduced in a volume of gas of low pressure, free electrons are accelerated and collide with neutral gas molecules. Following the collision, dissociation, ionization or excitation can happen. Through dissociation (see Figure 1.2), gas molecules are broken down into smaller fragments called "Free Radicals":

$$M + e^- \Rightarrow M1 + M2 + e^-$$

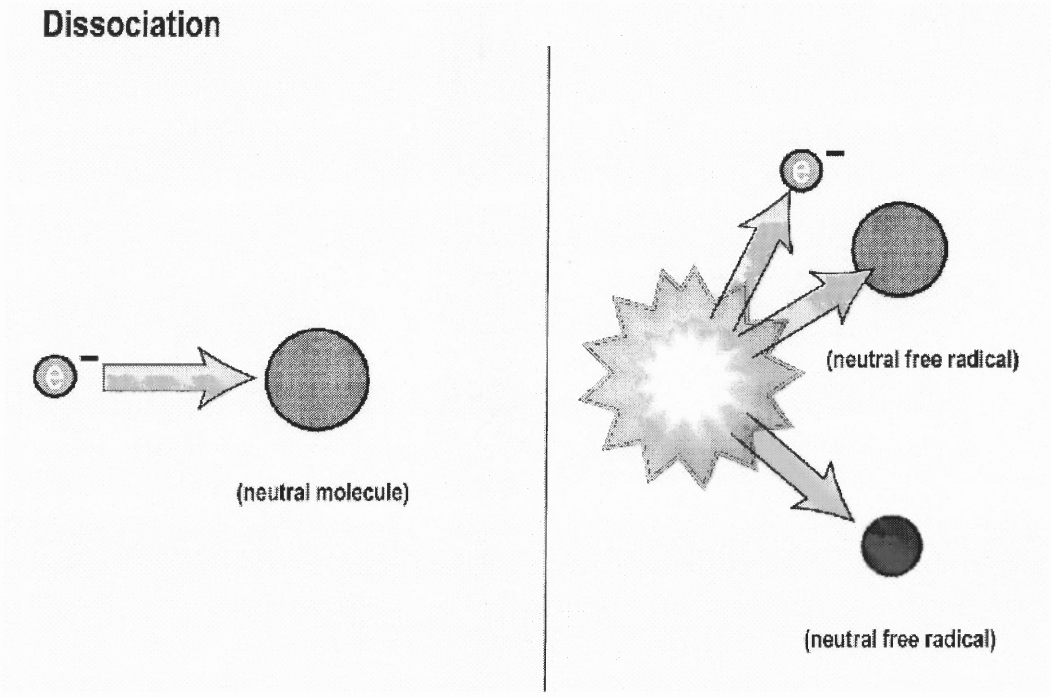


Figure 1.2 Schematic of dissociation.

These free radicals are electrically neutral, highly reactive, unstable chemical species. They readily react with other substances in order to achieve a more stable configuration.

The most important parameters that affect generation of free radical as well as ions are the voltage and gas pressure.

**Plasma Ignition**

The relationship between pressure and DC ignition voltage is called the "Paschen Curve" (Figure 1.3). There is a pressure "sweet spot" at which the voltage for striking plasma has a minimum.

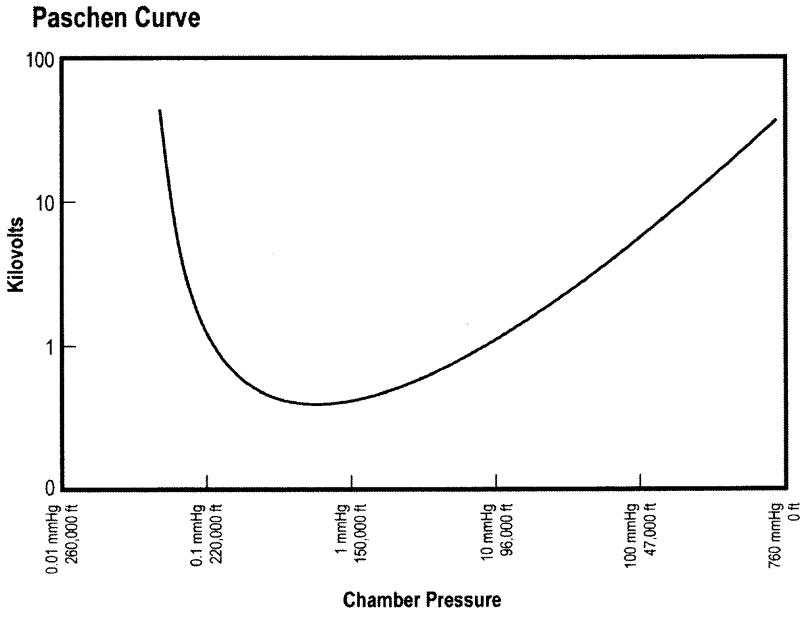


Figure 1.3 Plasma ignition paschen curve. [7]

In DC Plasmas, the glow discharge divides itself into glow regions and dark spaces between the cathode and the anode as shown in Figure 1.4(a). When the two electrodes are brought together, the cathode dark space and negative glow are unaffected whilst the positive column shrinks. The minimum separation is about twice the dark space thickness, at less than this, the dark space is distorted and then the discharge is extinguished [8].

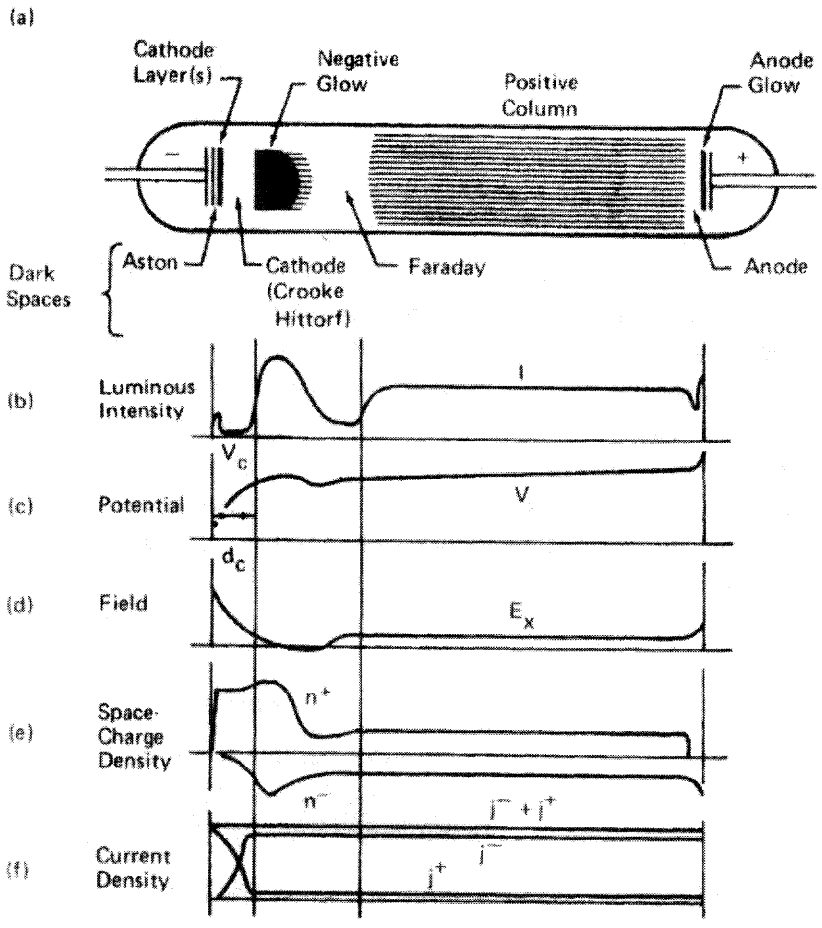


Figure 1.4 The normal glow discharge in neon in a 50 cm tube at P = 1 torr. (the luminous regions are shown shaded). [8]

Figure 1.4 also shows the distribution of luminous intensity (b), potential (c), electric field (d), space charge density (e) and current density. Since current must be continuous in a system, it is clear that the currents at the two electrodes must be equal. The voltage distribution in a DC glow discharge is shown in Figure 1.5, which demonstrates that the most of the potential change occur near the cathode, where ions are accelerated and that the plasma region between the cathode and the anode sheaths is more positive than the electrodes. The plasma region is also more positive than any object inserted into the system.

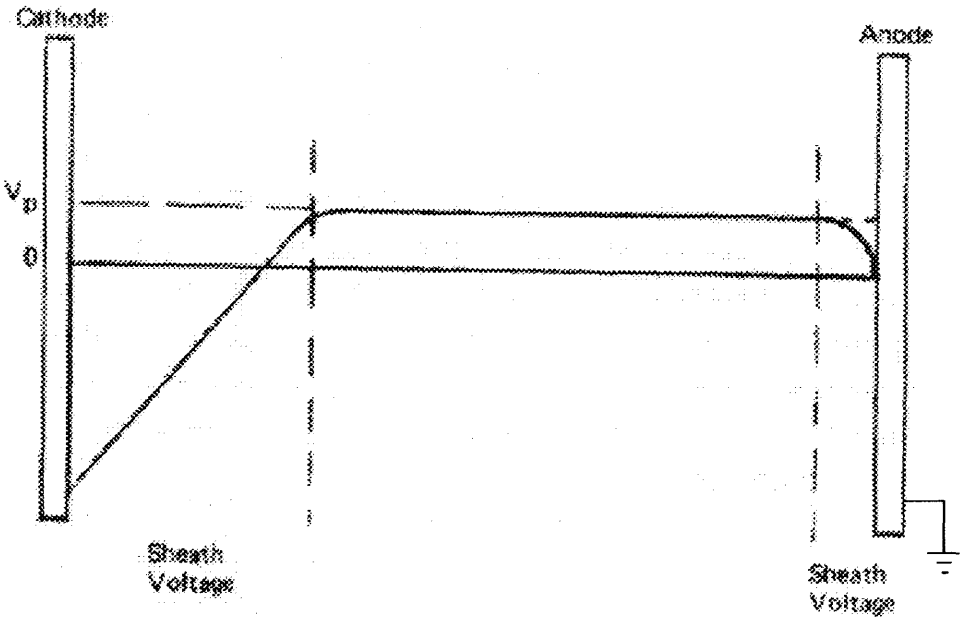


Figure 1.5 Voltage distribution in a dc glow discharge process (grounded anode). [8]

**Some Theoretical Considerations about PECVD of Carbon Films**

Plasma power plays a crucial role in formation of carbon film structure. Bubenzer et al. Proposed [9] that ion energy could be calculated from the bias voltage and pressure by the relation:

$$E = (K_2 B_b) / P^m; \quad 0 \leq m \leq 1$$

Where $K_2$ is constant, $B_b$ is the voltage, $P$ is the total deposition pressure and $m$ is a coefficient.

At low voltage, polymer-like films with a high fraction of hydrogen and fully saturated $sp^3$ groups can be deposited.

Increasing voltage leads to the increase of ion energy as the deposition pressure is constant, depletion of hydrogen and promotion of the formation of a rigid carbon

network due to the subplantation of the incoming radical into the first atomic layers [9].

Etching of the deposited film by sputtering effect of argon ion also plays a role due to the high flux energy and mass of argon ion in the plasma, especially at increased power. If we take into account the small binding energy of the physisorbed radicals in the absorption layer, it becomes clear that the sputtering effect of energetic argon ions will be very important.

The net deposition rate of carbon films may be expressed in a general manner [9] by

$$r = r_a - r_e - r_s$$

where $r$ is the net deposition rate of carbon films, $r_a$ is the adsorption rate of carbon radicals, $r_e$ is the etching rate of carbon radicals, and $r_s$ is the sputtering rate of the film by argon ions.

The deposition rate is proportional to the power and total pressure at lower voltage and pressure range.

Part of the physisorbed radicals can be transferred to the chemisorbed state by impact of energetic particles (ion-induced stitching).

This model [9] was successful in describing the temperature and gas flow dependence of the deposition rate, as well as the composition of the deposited films.

### 1.2.3 Deposition Mechanisms

**Growth and Nucleation Mechanism**

The modeling of the deposition process has been widely studied by many authors on the basis of theoretical considerations and experimental results.

Deposition mechanisms essentially concerns a condensation on a solid surface, i.e. nucleation and growth mechanisms: [4] [10]

1. Chemisorption or growth mechanism: depends on the availability of active sites. Radical processes are favored, the active species are essentially free radicals, which are unstable (life-time less than about 0.01 s). Side products are stable molecules, not transformed into solid carbon.

2. Physisorption or nucleation mechanism: depends on polycyclic aromatic hydrocarbons which are large enough to be physisorbed. These are fundamental for the rate of formation of carbons. These interfacial reactions associated with a sticking coefficient and surface migration specific for each species, are very difficult to analyze and therefore to control. The influence of 'catalysts' such as transition metals or an additive reacting gas are also predominant factors.

The substrate plays a role in the first film layers from a physical (roughness, curvature and surface energy) and a chemical (nucleation sites) point of view. The basic thermodynamic approach for a hemispheric nucleus indicates that the Gibbs enthalpy for heterogeneous nucleation is always lower than for homogeneous nucleation [4].

A nucleation process is determined by the physisorption of relevant species on the surface. Therefore, adsorption equilibrium is important, whereas active sites are not needed. The nucleation mechanism is limited to large and very large polycyclic aromatic hydrocarbons [10].

This shows that a growth mechanism and a nucleation mechanism were clearly distinguished. The individual processes are a function of the geometry of the deposition apparatus defined by the ratio of the substrate surface area and the free reactor volume.

**Radical Reactions**

Generally speaking, the degradation and polymerization of aromatic monomers can be divided into three reactions: Diels-Alder, benzyne and radical reaction. [11]

Radical reaction has been observed in reactions of aromatic compounds, such as naphthalene, acetophenone and anthracene.

Radicals are species with at least one unpaired electron which, in contrast to organic anions or cations, react easily with themselves in bond forming reactions. In the liquid phase most of these reactions occur with diffusion controlled rates. Radical-radical reactions can be slowed down only if radicals are stabilized by electronic effects (stable radicals) or shielded by steric effects (persistent radicals). [12]

The fact that reactions between radicals are in most cases very fast could lead to the conclusion that direct radical-radical combination is the most synthetically useful reaction mode. This, however, is not the case because direct radical-radical reactions have several disadvantages. Nevertheless, there are useful synthetic applications [12] in which new bonds are formed from radical-radical combination.

The second method for the synthesis of products using radical chemistry employs reactions between radicals and non-radicals.

A radical chain is built up by different types of propagation steps all of which lead to new radicals: [12]

- Addition reactions: $R^{\cdot} + AB \Rightarrow RAB^{\cdot}$
- Substitution (abstraction) reactions: $R^{\cdot} + AB \Rightarrow RA + B^{\cdot}$
- Elimination (Fragmentation) reactions: $RAB^{\cdot} \Rightarrow RA + B^{\cdot}$

- Rearrangement reactions: $RAB^{\cdot} \Rightarrow ARB^{\cdot}$
- Electron transfer reactions: $R^{-} + M^{n+} \Rightarrow R^{\cdot} + M^{(n-1)+}$ or

$$RX^{\cdot} + RY \Rightarrow RX + RY^{\cdot -}$$

Carbon-centered radicals exhibit high chemoselectivities and their use in reactions with complex molecules may be important.

Vapor-phase polymerization of 3,4,9,10 perylenetetracarboxylic dianhidride (PTCDA) proceeded by a radical reaction of perylene-tetraradical and 3,4-perylenedicarboxylicanhydride-diradical. Since the biradicals are separated from each other by the tetradic carbon, they can exist rather stably and the benzyne or Diels-Alder reaction is prevented [11].

## 1.3 Polymeric Carbon Films

### 1.3.1 Precursors

The different types of allotropic forms of crystalline and non-crystalline carbon are essentially a function of two basic parameters: the nature and phase of the precursor and the experimental route selected to deliver the process energy.

There are two main classes of precursors: pure solid carbohydrates or various gaseous and liquid hydrocarbons, possibly containing hetero-elements such as oxygen, nitrogen or halogens [4]. In the first case, physical processes such as thermal evaporation or laser beam deposition, or sputtering are used. In the second case control of the complex and numerous chemical reactions is essential.

Starting from a hydrocarbon precursor, rather complex chemical processes occur,

including pyrolysis and carbonization steps to obtain a pyrocarbon coating. Polycyclic aromatic hydrocarbons (PAHs) are proposed as a carbon source for the fibrous product [13]. The carbons formed from the pyrolytic conversion of organic compounds are shown to consist exclusively of hexagonal structure units exhibiting varying degrees of cross linking.

Aromatic molecules (benzene and derivatives) decompose at a lower temperature than the alkanes (such as methane or propane).

In this project PTCDA has been used as the precursor. Side groups of large-sized condensed aromatic compound such as PTCDA and PTCDI have a function of protecting of the condensed aromatic rings [6] [14]. The distance between the molecular planes within the one-dimensional stacks (3.37 Å for PTCDA) is small in comparison with other lattice constants and also small in comparison with the size of the molecules [15]. This causes strong interactions of the $\pi$-electron systems within the stacks, but a very weak interaction in the other directions.

Some data on PTCDA are listed in APPENDIX B

Perylenetetracarboxylic monoimides and diimides themselves are very interesting photoactive and electroactive organic materials. These materials are being investigated for use in a variety of technological applications such as photoreceptors and electroluminescent displays [16].

Figure 1.6 shows the structure of perylene tetracarboxylic monoimides and bisimides. The RR compounds have $D_{2h}$ symmetry and the $R_1R_2$ compounds have $C_{2v}$ symmetry.

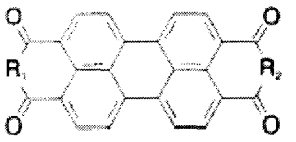


Figure 1.6 General structure of perylene tetracarboxylic monoimides and bisimides.

The molecular orbital (MOs) frontier region is formed by orbitals located on the perylene skeleton. It is also found that the various alkyl substituents (R) have little influence on the frontier MO region. [16] Quantum chemical calculations for PTCDA give smaller relaxation energies of 72 meV (cation) and 127 meV (anion) compared to 323 meV for the excited singlet. [15]

Figure 1.7 shows charges and bond orders for PTCDA.

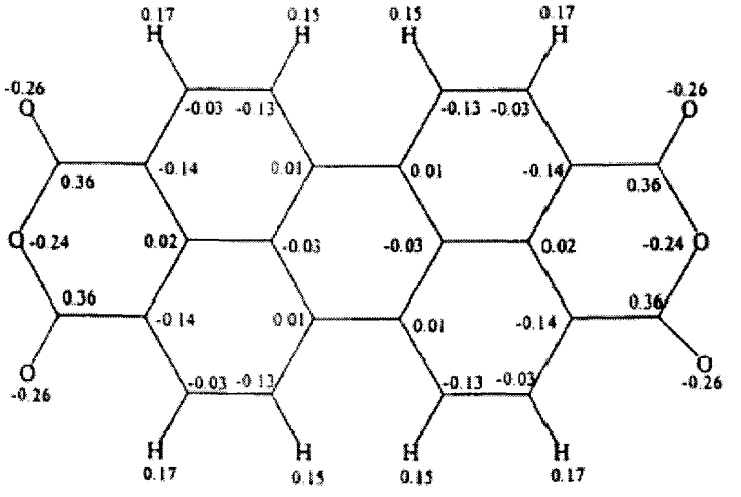


Figure 1.7 Charges and bond orders for PTCDA. [16]

It was found that the perylene moiety preserves much of its characteristic electron density distribution.

PTCDA weight-lose started at 490°C and 65% of PTCDA was evaporated when the temperature reached 570°C [11]. Since the temperature is nearly equal to the temperature at which the fiber formation started, the reaction is thought to proceed in the vapor phase.

### 1.3.2 Films with Poly-peri-naphthalene (PPN) Structure

**Introduction to PPN**

Poly-peri-naphthalene (PPN) film is well known as one of the low-dimensional conducting polymers. Highly electrically conductive polymers, also called synthetic metals, combine the electric properties of metals with the advantages of polymers such as smaller weight, greater workability, resistance to corrosion and lower cost. The hydrocarbons with ladder structure play a very important role among these materials; one member of this family is poly-peri-naphthalene (PPN). [17]

One-dimensional (1-D) graphite polymers have been expected to have distinguished physical properties because of their unique molecular structure lying between polyacetylene and graphite. [11]

Conjugated polymers with fused rings are especially appropriate in order to achieve low band gap (Eg) values, large bandwidth (BW) values, and low ionization potentials (I.P.) (4.08 eV [14]). However, high molecular weight polybiphenylene appears quite difficult to synthesize. This is also the case for simpler fused-ring systems. In this context, Poly-peri-naphthalene is noteworthy, since a synthesis route is available to produce a form of this polymer – albeit one which may involve

important chemical irregularities. [18]

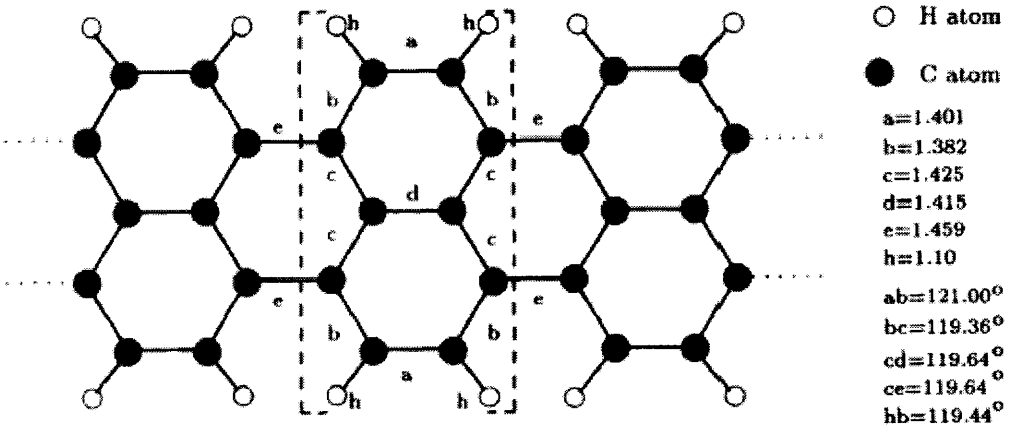


Figure 1.8 PPN geometry.
(bond distances are given in Å, bond angles in degree, the unit cell is denoted by a dashed bracket.) [17]

PPN geometry is shown in Figure 1.8, PPN chains stacked coplanarly in a layer, the separation between each layer being about 3.55Å. PPN should have high thermal stability as a consequence of the retained benzenoid character. [19]

Bogar [17] calculated a gap value of 1.06 eV for PPN and 4.45 eV for PPP using Clementi's double zeta basis (DZ). According to the relation $\Delta E_\infty = [\Delta^2_{geom} + \Delta^{2.5}_{corr}]^{\frac{1}{2.5}} = 1.2\,eV$. The result is in good agreement with the experimental evaluation of $\Delta E_\infty$ = 1.3 eV obtained by means of extrapolation of the experimental data reported by Müllen *et al.* [20] Figure 1.9 is band structure of PPN.

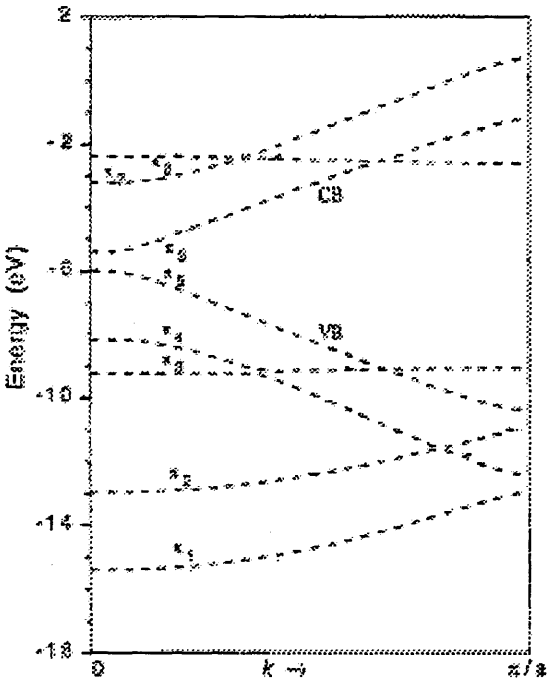


Figure 1.9 Band Structure of PPN.
(only $\pi$ bands are displayed.)[21]

**Literature Review**

Deposition technology and mechanism has been widely studied by many authors on the basis of theoretical considerations and experimental results.

**I. Kaplan et al.**

Kaplan et al. [18] found that pyrolysis (>700C) of PTCDA in an evacuated system results in the loss of hydrogen, CO and $CO_2$ and the deposition of a chemically inert, metallic-appearing mirror-like film. The films are highly conducting and can evidence either metallic or semiconducting behavior, depending on the preparation temperature. The properties of typical films they got are

1. $\sigma_{RT}$=250 $\Omega^{-1}$ $cm^{-1}$ at room temperature.

2. C/H=12/1;
3. Increased ordering in the [001] direction compared with diamond and graphite. X-ray diffraction analysis yields no diffraction lines;
4. TEM examination indicates a lamellar structure (a layered type structure), where each layer is composed of polycrystalline or amorphous material. This is quite unlike turbostratic carbons commonly formed in pyrolytic procedures;
5. Auger analyses reveals it to be extremely clean except for small amounts of oxygen, phosphorus and sulfur;
6. The density was 1.758g/ml;
7. The index of refraction was n=2.86 and k=1.65;
8. The films are exceptionally resistant to chemical attack;
9. Have the characteristic of a highly delocalized spin system.
10. The exciton-phonon coupling constant g = 2.0025 (2.0028 [14], 0.84 for PTCDA [15])

The authors thought a formulation including PPN units would be quite reasonable for their films.

**II. Kamo et al.**

In Kamo and coworker's [22] opinion, pyropolymers are known to have remarkable thermal stability and high electrical conductivities without doping. It is exceedingly difficult to realize the required chemical structure of the polymer chains and the highly ordered aggregation states. An exceptional pyropolymer is PPN made by gas phase polymerization of PTCDA around a narrow temperature range near 500°C. At these temperatures, only dianhydride groups are removed from the PTCDA molecule and polymerization proceeds selectively along the longer chain direction, that is, one-dimensionally. Fiber-like PPN with amorphous structure was

obtained by CVD using PTCDA as a source material. The temperature of PTCDA and Fe substrate was kept at 520 and 380°C, respectively. They found that hydrogen atoms remain in the film but the dianhydride groups are lost at 520°C (quadrupole mass spectroscopic observation). They also found that no sharp peak of Raman spectra is observed of the material deposited at 300°C. Its chemical structure is not clear, but it is not PTCDA because the strong intensity due to the luminescence of PTCDA does not appear in the Raman scattering spectrum.

They concluded that:

1. A probable mechanism for PPN film formation from PTCDA by CVD is that PTCDA is pyrolyzed at 520°C, loses the dianhydride groups, changes to perylene radicals and deposits as a precursor of PPN on the substrate.

2. A long lifetime of perylene radicals and the catalytic effect of Fe are thought to be responsible for the successful formation of PPN films.

3. The smaller electrical conductivity and the larger activation energy of the film made at 380°C compared with those of the fiber indicate less defects and /or impurity in the PPN films grown by CVD.

**III. Murakami**

Reference [11] concerns the morphology and polymerization mechanism of PPN. Murakami synthesized PPN fiber from PTCDA that was heated in Ar or $Ar/H_2$ gas with an infrared radiation furnace. Very fine fibers, which have rectangular cross sections of 0.1 to 0.4 μm on sides with length up to 10mm, were grown at Tp higher than 520°C in argon. Thermogravimetric curve indicates that the precipitate consisted of three components: Perylene, PDCA and PTCDA. Thus the decomposition reaction of PTCDA is ascribed merely to the scission between perylene and carboxylic

dianhydride groups. The reaction is thought to be proceeded by perylene tetra radicals and 3,4-perylene dicarboxylic anhydride biradicals. Figure 1.10 summarizes the polymerization mechanism of PTCDA.

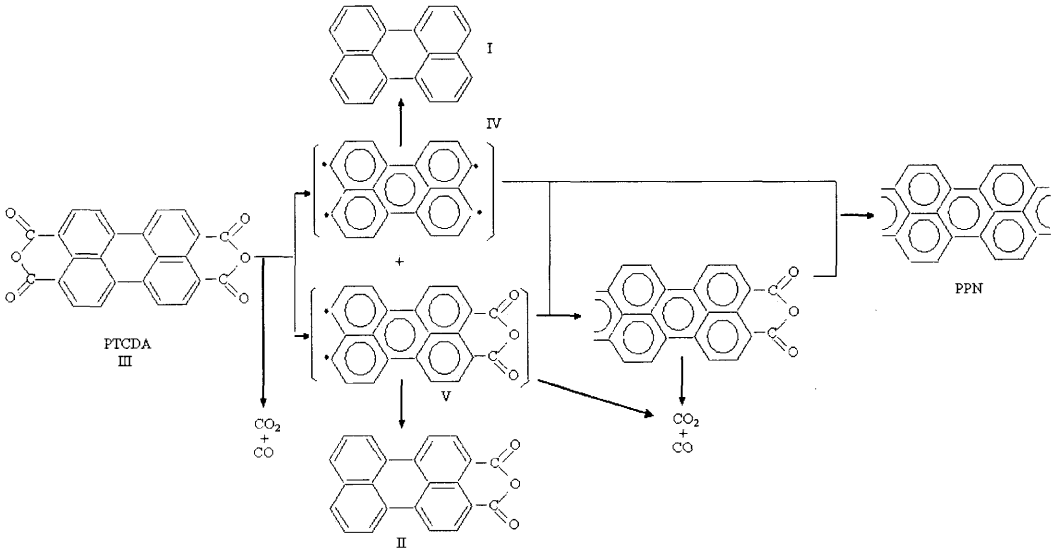


Figure 1.10 Polymerization mechanism of PTCDA. I: Perylene, II: PDCA, III: PTCDA, IV: Perylene radical, V: PDCA radical.

PPN fiber synthesized in Ar had a rectangular cross section and that in $Ar/H_2$ had a flat ribbon like morphology. The morphology of the fibers is determined by the reaction intermediates and is not inherent to the PPN structure.

**IV. Tanaka et al.**

Tanaka et al. [14] have prepared homogeneous semiconductive organic thin films by the radio frequency plasma polymerization of PTCDA. They found that with rf plasma power 10W, obtained films showed the conductivity of $1.0\times10^{-1}$ S/cm at room temperature (same value in references [23], The room-temperature electrical conductivity of the PPN polymer was 0.2S/cm along the fiber axis and that of

graphitized PPN was 8000S/cm. [24]). This polymerized product was an n-type semiconductor, the temperature dependence of it's conductivity can be well explained by the 3D variable range hopping mechanism. Perylene monomer having no side groups attached to the condensed aromatic rings was found to be easily destroyed in the plasma atmosphere. They think the sort of the side groups and the size of the condensed aromatic rings of the starting monomer hold the key to obtain the sample with higher conductivity.

Additionally, it was found that the conductivity decreased upon exposure to air, probably due to compensation effect to the conduction carriers or scavenging the dangling bonds to impede the conduction paths by oxygen.

**V. Murashima et al.**

Murashima et al. [6] studied the influence of plasma polymerization conditions and surface composition on electrical conductivity of plasma polymerized PTCDA thin films. The polymer produced has highly cross-linked structures of carbon bonds developed with the destruction of the aromatic ring in the plasma atmosphere.

The electron spectroscopy for chemical analysis (ESCA) measurements have suggested a possible important role for nitrogen when it is used as a carrier gas. The nitrogen may be incorporated in the skeleton of the samples and cause an increase in the electrical conductivity, as can be expected from theoretical considerations on "intrinsic doping" of organic semiconductors with nitrogen or boron atoms.

**VI. Bredas and Baughman**

In order to understand the origin of high conductivities observed for a pyrolysis

product which contains PPN chains, Bredas and Baughman [19] have investigated the electronic properties and crystal structure of PPN by combining the quantum chemical valence effective Hamiltonian (VEH) technique and crystal packing methods.

VEH (valence effective Hamiltonian technique) band structure calculations for an isolated PPN chain predict a band gap which is small, 0.44 eV. [17] [19] The highest occupied and lowest unoccupied (HOMO and LUMO) bands have a combined width of about 9 eV. [17] VEH results strongly suggest that PPN is not an intrinsic metal. This is consistent with the fact that the conductivities at room temperature reported for nongraphitized PPN are of the order of $10^{-2}$-$10^{-1}$ S/cm [19].

Crystal packing analysis predicts the existence of two phases for PPN, a phase in which PPN molecules are arranged as overlapping dimmer pairs and a nondimeric phase in which there is little intermolecular overlap.

The observed diffraction patterns for PPN suggest the packing of overlapping molecules in a third type of structure, possibly stabilized by a degree of irregular reaction during synthesis. Quantum chemical calculations indicate that interchain overlap decreases the band gap of PPN, from 0.44 eV for the isolated chain to 0.29eV. (0.38eV [17])

Using the quaterrylene ($C_{40}H_{20}$) structure as a model for PPN: the unit cell is monoclinic, $P2_1/a$, with four monomer units (4 $C_{10}H_4$ units) per unit cell and a=11.14Å, b=10.63Å, c=4.32Å (chain axis), and $\beta$ = 91.5°. The corresponding calculated density ($\rho$) is 1.61 g/cm$^3$.

## 1.4 Project Goals

The aim of this project was to synthesize PPN films in an efficient way of a relatively low temperature by PECVD and CVD of PTCDA .The specific goal was to determine the range of growth conditions that produce high quality PPN films.

The project consisted of the following tasks:

1. Design and construct a deposition system, capable to perform PECVD and CVD of high quality carbon films with PPN structure.

2. Determine deposition conditions, e.g., partial pressure of precursors, flow rates, temperatures, nature of substrates, plasma power etc.

3. Evaluate films and provide information for further development

Task 1 and 2 are described in chapter 2, and the results of the film evaluation in chapter 3 and chapter 4.

# CHAPTER 2

# DEPOSITION PROCEDURE

## 2.1 Setup of the Vacuum System for the Deposition

The synthesis of the carbon films was carried out in a PECVD system built in the ion beam and thin film laboratory of NJIT. Building our own vacuum system offers many advantages over purchasing a pre-designed or custom-built system. There are some points to keep in mind when designing and constructing this system: [26]

1. Application specific: Systems can be designed using UHV components or lower-cost HV components, depending on the application.

2. Versatility: Using standard components instead of custom parts ensures easier, more versatile upgrades at a later date.

3. Compatibility and reliability: Buying from a single source ensures component compatibility. Buying from a company experienced in vacuum system design and construction ensures reliable component performance.

4. Lower costs: Buying individual components can cost less than buying an integrated system.

The deposition system design integrates a glass tube, adaptors, electrical feedthroughs, thermocouple, pump, pressure gauges, heating lights, valves, DC plasma power supply, argon gas source, mounting frames, service components (such as power distribution).

The following major components were used in construction of the system:

1. Pressure meter: MKS INSTRUMENTS INC. PRESSURE TRANSDUCER TYPE 122A
2. Pump: L-H TRIVAC DL6A;
3. Thermocouple meter: OMEGA 4002A-T;

4. DC. Power Supply: ADVANCED ENERGY INDUSTRIES, INC, MDX MAGNETRON DRIVE;
5. Flow Rate Meter: DATAMETRICS, type: 1511 CONTROLLER;
6. Pressure Meter: DATAMETRICS, type: 1500;

Heating of the substrate and the source was accomplished by the use of halogen lamps (two 500 watts lamps for the source, one 500 watts lamp for the substrate).

Structural diagram of the deposition system is shown in Fig 2 -1.

The process chamber is a glass tube of length 78cm with the inner diameter of 3.81cm, mounted into compression type vacuum fittings. The distance between the source and the substrate was approximately 15cm. Steel substrates were placed horizontally on an aluminum holder, to which a thermocouple that was isolated from the ground was attached.

Argon gas was introduced into the tube as a carrier gas. The flow rate of argon gas was controlled and measured by the DATAMETRICS flow rate controller when 10sccm and below was required.

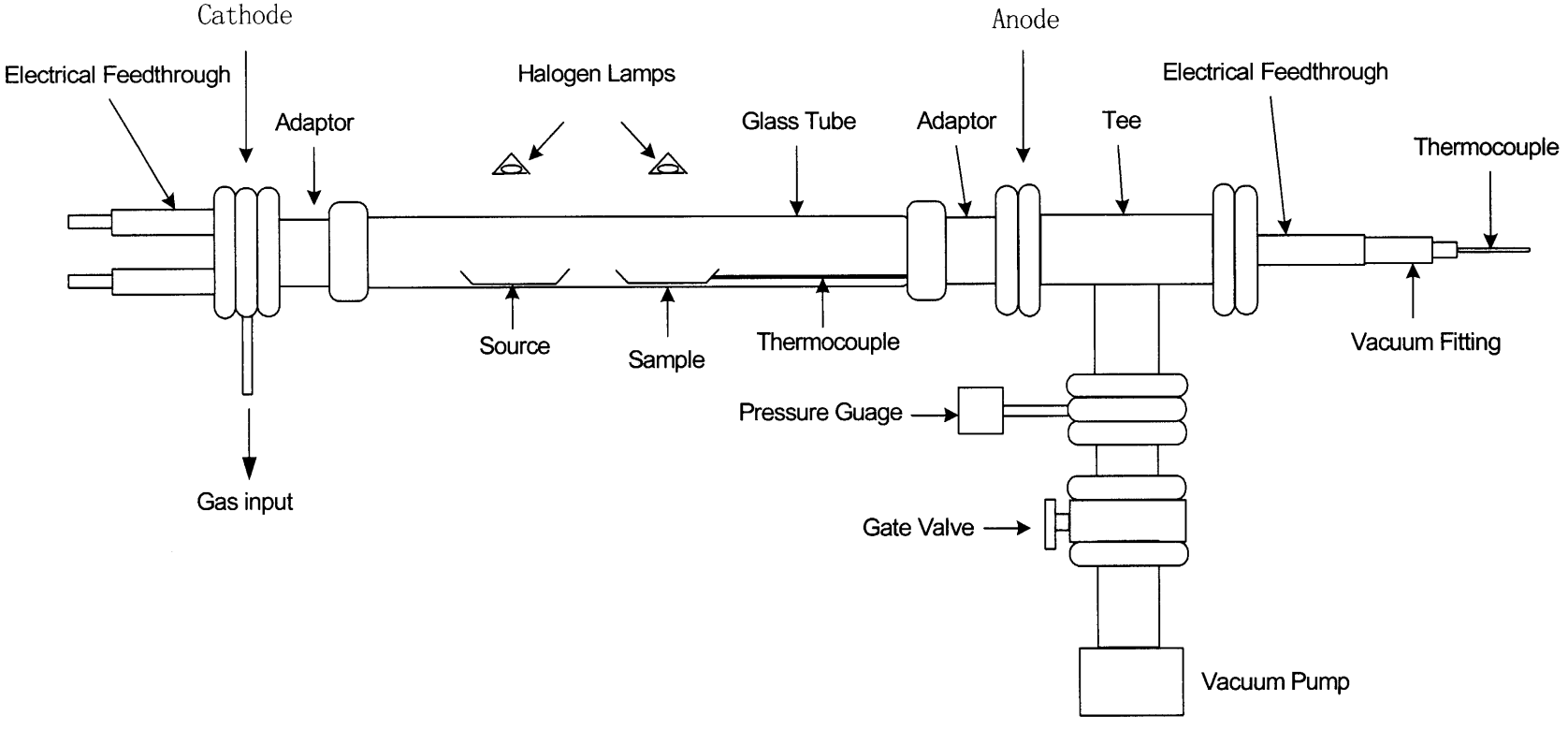


Figure 2.1 Schematic of the deposition system.

## 2.2 Characterization of the D.C. PECVD System

### 2.2.1 Gas Flow and Pressure Drop Across the Tube

**Gas Flow**

Gas flow regimes are characterized by the nature of the gas and by the relative quantity of gas flowing in a pipe. The nature of the gas flow is determined by examining Knudsen's number:

$$Kn=\lambda/d$$

where d is a characteristic dimension of the system (diameter of the tube), $\lambda$ is the mean free path:

$$\lambda= 1/(2^{1/2}\pi d_0^2 n)$$

where $d_0$ is the molecular diameter in meters (for argon, $d_0$=0.364nm), $n$ is the gas density in molecules per cubic meter.

According to $P = nkT$ one can get $n$, if $n$ is expressed in units of $m^{-3}$, $k$ (Boltzmann's constant) in joules per Kelvin ($1.38\times10^{-23}$ J/K), and T in kelvins, the P will be given in units of pascals (Pa). In the experiments pressure range was around 1 torr/133.322 Pa, the degree of vacuum is medium.

In room temperature (T~300K):

$$n = 3.2\times10^{22}\ (m^{-3}),\ \lambda = 0.052mm,\quad \text{so } Kn=\lambda/d \approx 0.001$$

when temperature increased to 400°C:

$$\lambda = 0.117mm,\quad \text{then } Kn=\lambda/d \approx 0.003$$

since the viscous gas flow characterized by Kn<0.01, the system operated in viscous regime.

The relative quantity of gas flowing in a pipe is described by Reynolds' dimensionless number:

$$R = U\rho d/\eta$$

where $\rho$ is the mass density ($kg/m^3$) of the gas of viscosity $\eta$ flowing with stream velocity U in a pipe of diameter d. For R>2200, the flow is turbulent; for R<2200, laminar.

For argon as carrier gas at flow rate 10sccm:

$$\rho = 39.95/22.414 = 1.78\ kg/m^3, \quad U = 10sccm/(\pi r^2) = 1.46\times10^{-4}\ m/s$$

where $\pi r^2$ is area of cross section of tube.

When temperature up to 400°C:

$$\eta = 0.499(4m\kappa T)^{1/2}/(\pi^{3/2}d_0^2) \approx 2.35\times10^{-9} Pa\cdot s$$

therefore, in our experiment $R=U\rho d/\eta \approx 4200$, so the flow is turbulent, but the value of R is very close to the value of laminar flow. Furthermore, because R is inversely proportion to $(T)^{1/2}$, R will further decrease at higher temperature..

**Pressure Drop Across the Tube**

The flow of gas in a channel is dependent on the pressure drop across the tube as well as the geometry of the channel. Intrinsic conductance of the channel is:

$$C = Q/(P_2-P_1)$$

where Q is throughput: the quantity of gas (the volume of gas at a given pressure) that passes a plane in a unit time. With flow rate of 10sccm, $Q=10cm^3/min\times1atm$ (1atm=760torr).

In viscous flow the gas conductance is a nonlinear function of the pressure drop in

the tube

According to "Nomogram for the evaluation of conductances of tubes of circular cross section (air, 20°C) in the total vacuum pressure range"[27], in our system, tube length is 78cm, the inner diameter of the tube is 3.81cm, when pressure is 0.8torr, the conductance C is 326.7 l/s, so:

$$(P_2\text{-}P_1) \approx 3.88 \times 10^{-4} \text{ torr}$$

therefore the pressure drop in the system between the outlet and the inlet is negligible comparing to the operating pressure.

A flow calibration has been measured beforehand. Figure 2.2 shows the corresponding real flow rate of dial reading of the argon gas.

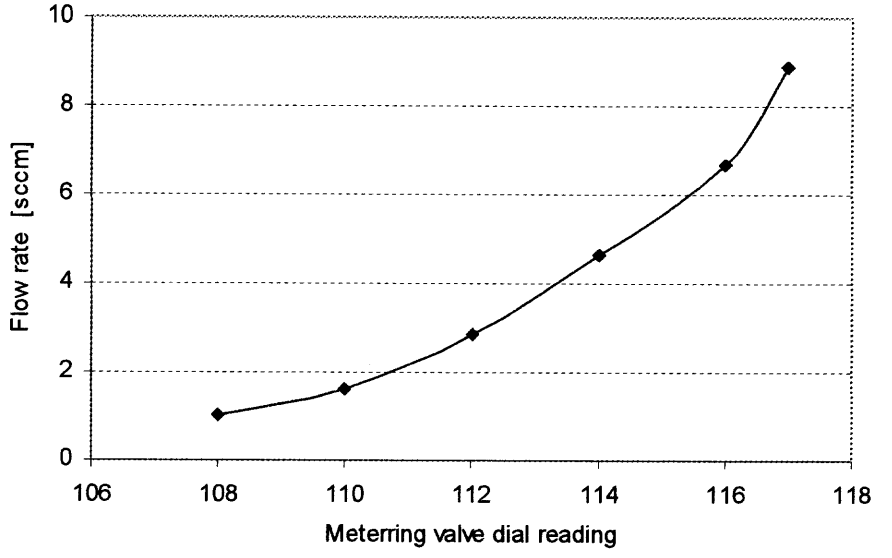


Figure 2.2 Flow rate calibration curve.

Accordingly Figure 2.2, dial reading of 117~118 correspond to 10sccm, 121 to 20sccm and 125 to 25sccm.

### 2.2.2 Plasma Characteristic

Plasma is sensitive to pressure and gas flow. The plasma condition has significant influence on properties of sample films. So an understanding of plasma parameters in our system is necessary for PECVD deposition of PPN films. Measured plasma properties will be used as data base for optimal process control. The results presented in this section were obtained with argon gas without the precursor vapor.

The electrical circuit of the deposition system is shown in Figure 2.3. The substrate was connected with a thermocouple, which was isolated from the anode and cathode but connected exteriorly to ground through a 400 Ω resistor or left floating. The voltage between the substrate and the ground (Vs) was measured with a digital voltammeter.

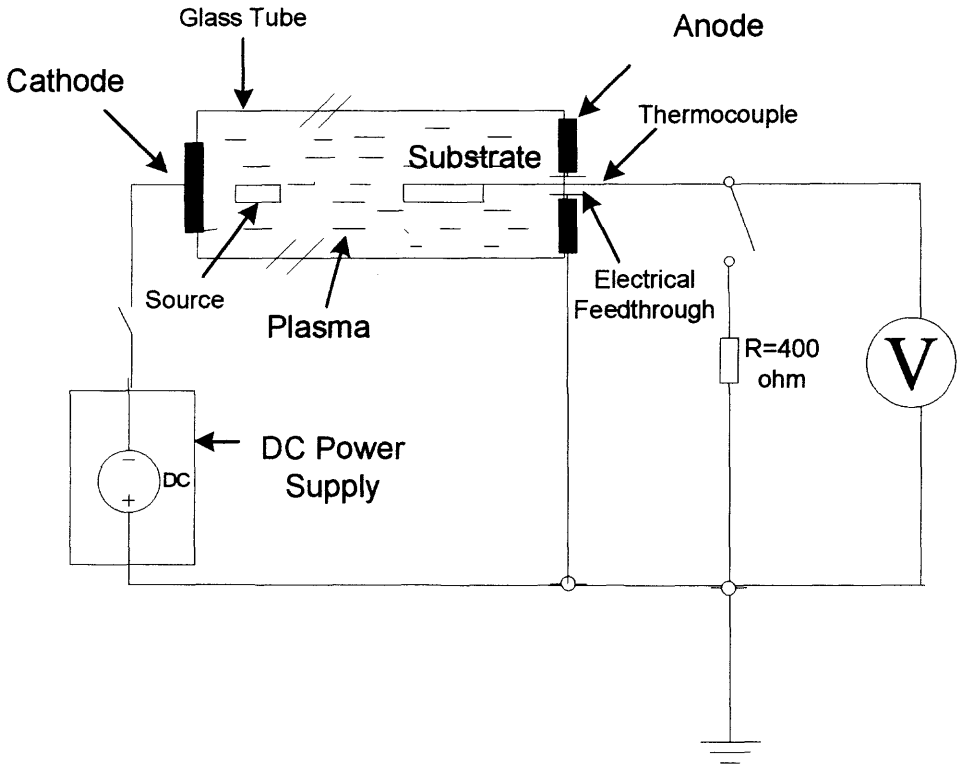


Figure 2.3 Circuitry schematic of the PECVD system

**Influence of Pressure:**

Voltage of the cathode (Vc) and substrate (Vs) was measured as functions of cathode current with constant flow rate (~11sccm) and the pressure ranges from 0.24 torr to 0.80 torr. Figure 2.4 and 2.5 show the I-V characteristic on cathode (Vc) and substrate (Vs) with and without a 400Ω resistance parallel connected with substrate.

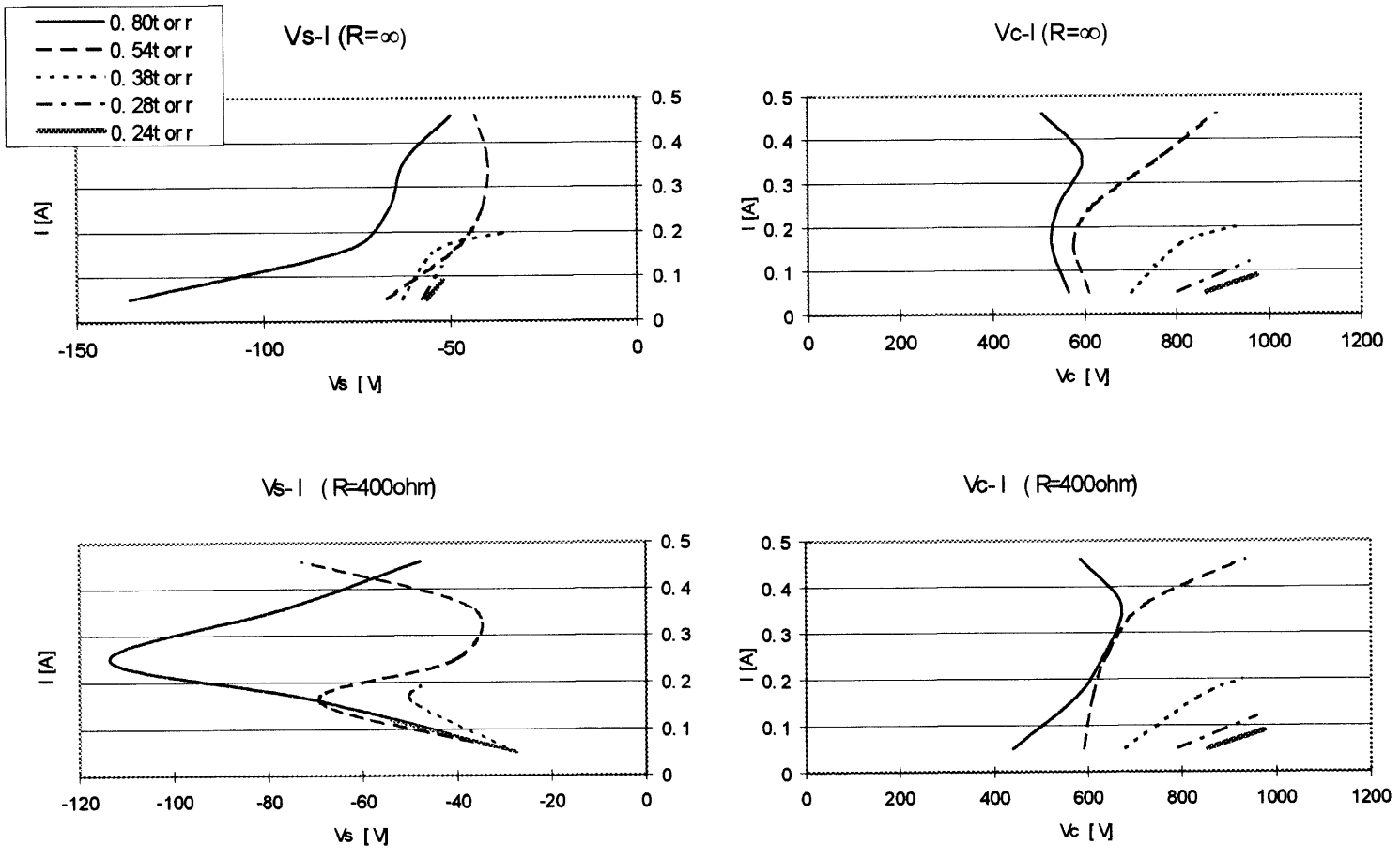


Figure 2.4 I-V curves of the plasma for different pressure (1)
(flow rate is 10sccm, R=400ohm indicates substrate parallel connected with a 400Ω resistance, R= ∞ indicates floating substrate.)

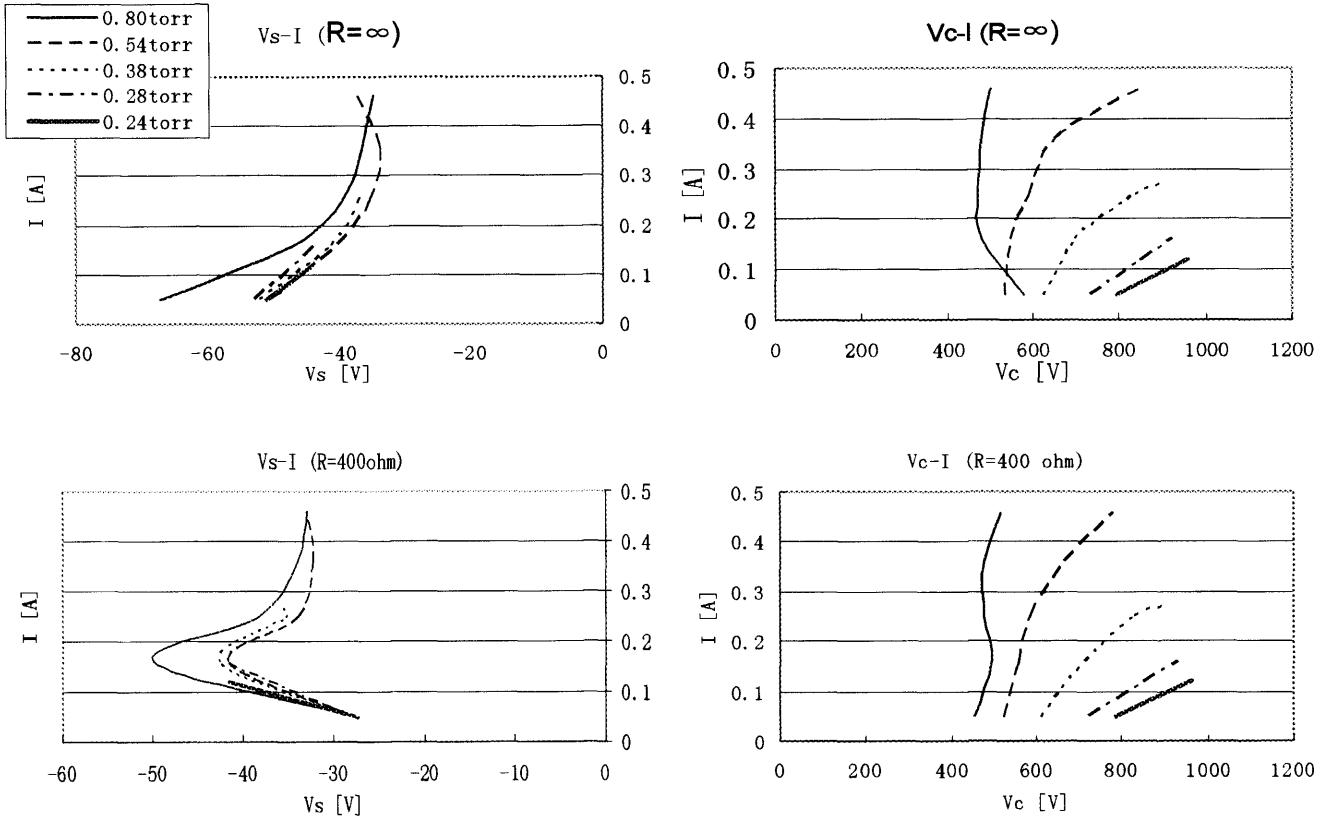


Figure 2.5 I-V curves of the plasma for different pressure (2)
(flow rate is around 22sccm, R=400ohm indicates substrate parallel connected with a 400Ω resistance, R= ∞ indicates floating substrate.)

Curves of Figure 2.4 and 2.5 are similar to the section between region 2 and region 3 of typical plasma's voltage and current characteristics (Figure 2.6)

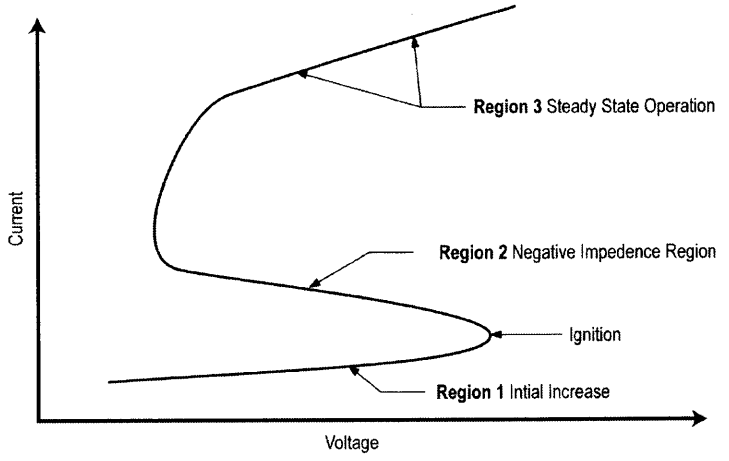


Figure 2.6 Voltage and current characteristics of plasma. [7]

Figure 2.4 and Figure 2.5 reveal that the influence of pressure on the electrical characteristic of the discharge is significant. The gas flow rate also influences the plasma condition, Figure 2.7 shows how I-V curves change with different flow rates for pressure of 0.8 torr.

(a)

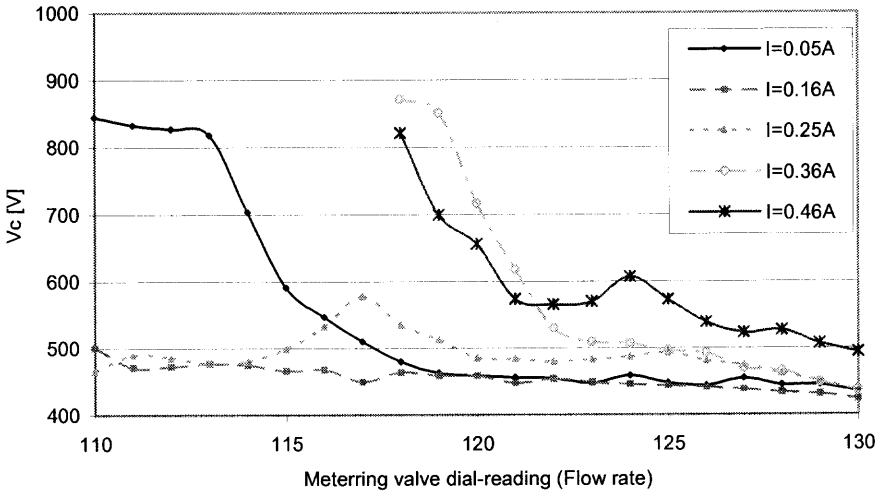


(b)

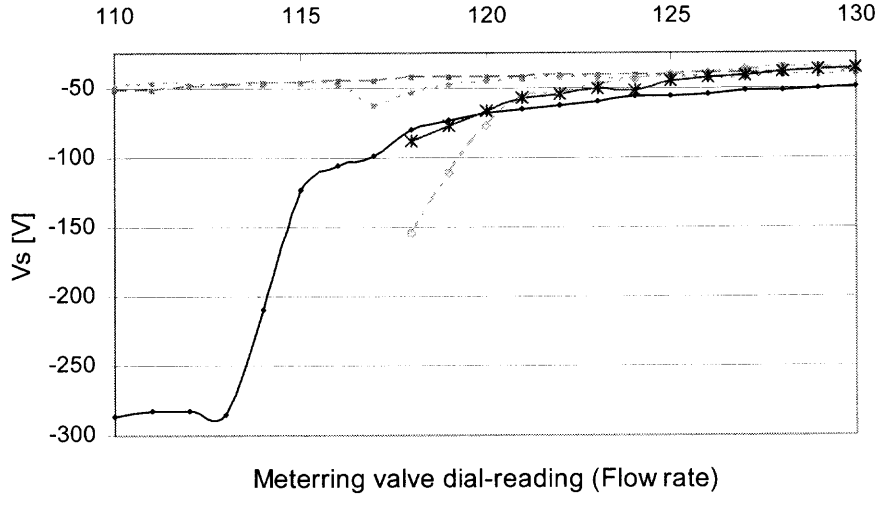


Figure 2.7 The cathode voltage (a) and the substrate voltage (b) as a function of flow rate for argon gas pressure of approximate 0.80 torr.

To obtain PPN structure, i.e., only to cleave side group of PTCDA (source) but not damage aromatic rings, low plasma energy is preferred, According to Figure 2.7 (a), for 0.05A current, lower voltage can be obtained at the current flow rate above dial-reading 118 corresponding to flow rate of 10sccm and above. According to

Figure 2.4 and 2.5, lower voltage can be obtained at pressure of 0.8 torr or above when current range from 0.05A to 0.46A. Therefore, in following conditions the low discharge energy requirement can be met: pressure of 0.8 torr or above, flow rate of 10sccm or above and current of 0.05A or below.

## 2.3 Deposition of Polymeric Carbon Films

### 2.3.1 Preparation of Substrate

The steel substrate is gun steel or stainless steel of 1.25cm×1.25cm square with thickness 0.15cm, the compositions shown in APPENDIX C.

Prior to loading the steel substrate, the substrates were cleaned using the following steps:

1. Abrasion: rubbed on 600 grit abrasive paper supported on a flat backing surface with water as lubricant;

2. Electrical-cleaning: concentration of solution, highly alkaline "59 special" made by North West Company, was 17gml/250ml, temperature was around 82°C, voltage was 7 volts, current was 0.08A/cm$^2$ and cleaning time was 15 minutes;

3. Ultrasonic cleaning: for 10 minutes in alcohol, then for 5 minutes in acetone and again for 10 minutes in alcohol

.

### 2.3.2 Deposition Procedure

For CVD process:

1. Mount cleaned substrate on aluminum substrate holder and connect thermocouple to the holder. Put them in proper substrate section of the clean glass tube.
2. Put the boats containing PTCDA in proper source section of the glass tube.
3. Seal the tube and pump the tube for 15 minutes with argon flow going through to purge the air from the system.

4. Turn off the pump, turn off the main gate valve, fill the system with Ar gas to atmosphere pressure and open the vent on the pump side of the tube.
5. Heat the substrate to pyrolysis temperature.
6. Heat the source (PTCDA) to sublimation temperature.
7. Continue the deposition for 3 to 4 hours.

For PECVD process:

1. Repeat steps 1, 2 and 3 above.
2. Adjust proper argon flow rate then adjust the main gate valve to get proper pressure in tube.
3. Heat the substrate to proper polymerization temperature.
4. Ignite plasma.
5. Heat the source to sublimation temperature.
6. Turn on and adjust the power supply and readjust the main gate valve to attain stable plasma condition with desired parameters (voltage and pressure)
7. Continue deposition for desired time or until the source be exhausted.

The most controllable and influential variables involved in the deposition process are:

1. The pressure in the tube;
2. The plasma conditions;
3. The discharge current;
4. The sublimation temperatures (the source);
5. The substrate's temperature;
6. The deposition time.

The results are presented and discussed in chapter 4.

# CHAPTER 3

# CHARACTERIZATION OF CARBON FILMS

## 3.1 Samples Deposited by CVD and PECVD

Many deposition runs were carried out with different settings of the variables in an attempt to achieve optimum deposition conditions.

Designations of the samples are as follows:

1. Suffix "-p" indicates samples that show characteristic PPN peaks in Raman spectrum;

2. COn (n is 1, 2, 3...): deposited by CVD in a tube of diameter 1 inch being heated by two-zone oven, this deposition system can be described as an atmosphere pressure hot wall reactor, it has uniform temperature distribution in the source and substrate area. All five samples prepared in this system shows PPN characteristic peak in Raman spectra, they are CO1-p, CO2-p... CO5-p.

3. CLn: deposited by CVD in the system shown in Figure 2.1 with source and substrates heated by hylogen lamps. The tube and the lamps were enveloped in Al foil. The vapor temperature in tube was not uniform. Samples CL5-p and CL7-p were deposited with some modification introduced to the system, they show PPN characteristic peak in Raman spectra. For CL5-p, the lamp irradiated the substrate surface on the film side; for CL7-p, the substrate was put in a copper tube (diameter 1 inch) inside the glass tube, so that copper tube rather than the substrate was directly heated by the lamps. In this case the conditions near substrate were close to those in a hot wall reactor, with vapor temperature close to the substrate temperature.

4. PLn: deposited by PECVD in the system shown in Figure 2.1. Among them PL5-p/Al has Al substrate which was radiantly heated from the film side directly on the surface. Samples PL4-p and PL5-p/Al has PPN characteristic peak in Raman spectra.

The following two tables give the summary of the samples obtained by CVD and PECVD respectively.

Table 3.1 Samples deposited by CVD.

| Sample | Flow Rate (sccm) | Pt | Ts (°C) | Tp (°C) | Dep. Time | Comments |
|---|---|---|---|---|---|---|
| CL1 | 10 | 5torr | 300 | ~400 | 30min | Almost nothing on substrate but deposition on tube wall |
| CL2 | 10 | 1atm | 350 | ~400 | 1h | Blue shiny film |
| CL3 | 10 | 1atm | 380 | ~400 | 2.3h | Blue and red mix, thin film |
| CO1-p | 10 | 1atm | 355 | 500 | 3.5 | Dark grey film |
| CO2-p | 10 | 1atm | 380 | 500 | 3.5h | Dark grey film |
| CL4 | 10 | 1atm | 380 | 510 | 3.5h | Dark grey and blue mix |
| CO3-p | 10 | 1atm | 380 | 510 | 3h | Thick black film with good adhesion. |
| CL5-p | ~15 | 1atm | 365 | 510 | 4h | Shiny blue thin film. The film side of the substrate was illuminated directly. |

Table 3.1 Samples deposited by CVD.
(Continued)

| Sample | Flow Rate (sccm) | Pt | Ts (°C) | Tp (°C) | Dep. Time | Comments |
|---|---|---|---|---|---|---|
| CL6 | 10 | 1atm | 375 | 510 | 3h | Dark grey. Reduced light intensity on surface of the film side during deposition. |
| CO4-p | 10 | 1atm | 380 | 520 | 3h | Green and brown mix |
| CL7-p | ~20 | 1atm | 380 | ~510 | 3h | Uniform dark grey film. Substrate in a copper tube |
| CO5-p | 10 | 1atm | 380 | 580 | 3h | Shiny black film |
| CL8 | ~25 | 1atm | 430 | 510 | 3h | Black and dark grey |
| CL9 | ~25 | 1atm | 470 | 510 | 4h | Dark red and black mix. Quite a bit dark red matter remained in source boat |
| CL10 | ~5.5 | 1atm | 470 | 510 | 4h | Thick dark grey film. Reduced light intensity on surface. |
| CL11 | ~5.5 | 1atm | 475 | 510 | 3.5h | As sample CL10. Reduced light intensity both on source and substrate. |
| CL12 | ~25 | 1atm | 500 | 510 | 4h | Dark grey, rough surface |
| CL13 | ~13 | 0.09torr | 516 | 400 | 30min | Dark grey, thin film |

Table 3.2 Samples deposited by PECVD.

| Sample | Flow Rate (sccm) | Pt | Ts (°C) | Tp (°C) | Ic (A) | Vc (V) | Is (A) | Vs (V) | Dep. Time | Comments |
|---|---|---|---|---|---|---|---|---|---|---|
| PL1 | 10 | 0.67torr | 300 | ~400 | 0.05 | ~720 | | | 1h | Very thin film |
| PL2 | ~25 | 0.7torr | 300 | ~400 | 0.05 | ~700 | | | 30min | Substrate is Si, very thin film |
| PL3 | 10 | 0.19torr | 380 | 350 | ~0.005 | 1023 | -16mA | 1.6~5V | 45min | Shiny blue and brown mix |
| PL4-p | 10 | 0.8torr | 350 | ~350 | 0.01 | 1023 | | | 20min | Thick black film. Scraped off easily. |
| PL5-p/Al | 10 | 1.2torr | 350 | ~400 | 0.03 | 1023 | | -450 | 30min | Glossy black film on Al substrate |
| PL6 | 10 | 1torr | 380 | 370 | 0.05 | 930 | | | 30min | Thick deposit, dark |
| PL7 | ~25 | 0.66torr | 300 | 510 | 0.05 | 760 | | | 30min | blue |
| PL8 | 10 | 1torr | 300 | 300 | 0.16 | 780 | | | 30min | Very thin film |
| PL9 | 10 | 1.3torr | 350 | 350 | 0.16 | 700 | | | 1h | Dark grey thin film |

Table 3.2 Samples deposited by PECVD
(Continued)

| Sample | Flow Rate (sccm) | Pt | Ts (°C) | Tp (°C) | Ic (A) | Vc (V) | Is (A) | Vs (V) | Dep. Time | Comments |
|---|---|---|---|---|---|---|---|---|---|---|
| PL10 | ~13 | 99mtorr | 380 | 400 | 0.16 | 500 | | | 30min | Black film with Bad adhesion |
| PL11 | 10 | 74mtorr | 260 | 350 | 0.25~ 0.35 | 480 | | | 30min | Brown thin film |
| PL12 | ~12 | 97mtorr | 500 | 350 | 0.26 | ~500 | | -125 | 45min | Thick dark green film |
| PL13 | 10 | 78mtorr | 530 | 400 | 0.36~ 0.46 | 430 | | | 25min | Brown thin film |

When the discharge energy is very high, black powder like soot arise around the source material (PTCDA). Whereas too low energy cause very thin film or fail to deposition. The black powder is supposedly carbon particles formed due to gas phase nucleation. Reducing pressure could minimize the gas phase nucleation. And it was suggested that gas phase nucleation could be minimized by reducing the flow rate. The optimum flow rate was found to be in the range of 10 to 30 sccm.

Some sample have poor adhesion but quite a number samples have fair adhesion. For stainless steel substrate and screw, all films have good adhesion. There is no evidence for void or bubble formation. [32] Aluminum foils that were put around the source be covered with uniform shiny black films.

Several samples have dull dark films. Most films on stainless steel substrate are shiny brown. Increase source's and substrate's temperature or increase plasma power could cause fracture of aromatic rings, carbon atoms would be deposited on the substrate and give the films black color.

The evaporation of the source material is very slow around 500°C. For PECVD, the deposition rate is increased significantly (to use up same amount of PTCDA, PECVD was 5~6 times faster and most PECVD films looks quite thick). In this PECVD system there is no means to measure the source's temperature, so the sublime temperature in Table 2.2 was by approximate.

Typical problems faced were: even Fe has good catalysis effects, the inner wall of the tube, especially the cold part and the part that around the source material, was covered with red and black stuff, respectively. It's found that cover substrate cause relative less deposition on tube wall.

## 3.2 Characteristic Test

### 3.2.1 Raman Spectroscopy

Raman spectroscopy has been well documented as a reliable method for analyzing the structure in carbon films [28].

The peak position in the Raman spectra yields information concerning the nature of bonding and bond-angle disorder [29]. For highly ordered single crystal graphite, there has a sharp graphite (G) peak at 1580 $cm^{-1}$ assigned to the high frequency basal-plane stretching mode of $sp^2$ bonded carbon atoms. Shift in the G band wave number is related to tensile and compressive stresses [28].

Major features in the Raman spectra of amorphous carbon films are the "G" mode (characteristic of intralayer vibration), and "D" mode (in microcrystalline and disordered graphite, 1350 $cm^{-1}$ peak) which is inactive for an infinite layer and is activated by the absence of phonon wave-vector (k) conservation, due to the presence of disorder [30]. The peak intensity is linearly related to the amount of crystal boundary in the sample [28]. In general, the position, widths, and relative intensities of these two features are found to vary with deposition conditions and film properties.

Films in this study are analyzed by two micro-Raman spectrometers, one is HORIBA/JOVIN-YVON LAB RAM system, cooled CCD, He-Ne laser of 632.8 nm wavelength. The other is a system with a 75 cm spectrometer equipped with a cooled CCD and using Ar laser at 514.5 nm as a source. The spectra were recorded over the range of 1000 -2000 $cm^{-1}$.

### 3.2.2 X-Ray Diffraction (XRD)

The principle of XRD measurement based on the interference of electromagnetic waves reflected from parallel planes of a crystal with spacing d, as is shown in Figure 3.1. When

$$d = \lambda / (2 \sin \theta),$$

the Bragg condition is satisfied and a peak will be measured in a detector scanned over angle 2 θ.

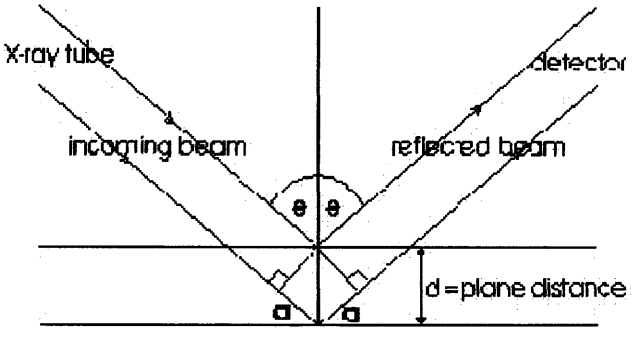


Figure 3.1 Principle of XRD measurements. [31]

X-ray diffraction patterns were recorded by a Philips X'pert MPK instrument with Cu $K_\alpha$ radiation (λ= 1.5418 Å ) with generator settings 40 mA and 45 kV. Intensity was recorded using continuous scan type and scan step time 0.8s from 2θ= 2° to 90°.

### 3.2.3 Scanning Electron Microscopy (SEM)

Scanning electron microscopy (SEM) is the best known and most widely-used of the

surface analytical techniques. SEM, accompanied by X-ray analysis, is considered a relatively rapid, inexpensive, and basically non-destructive approach to surface analysis.

Figure 3.2 shows the principle of SEM measurement

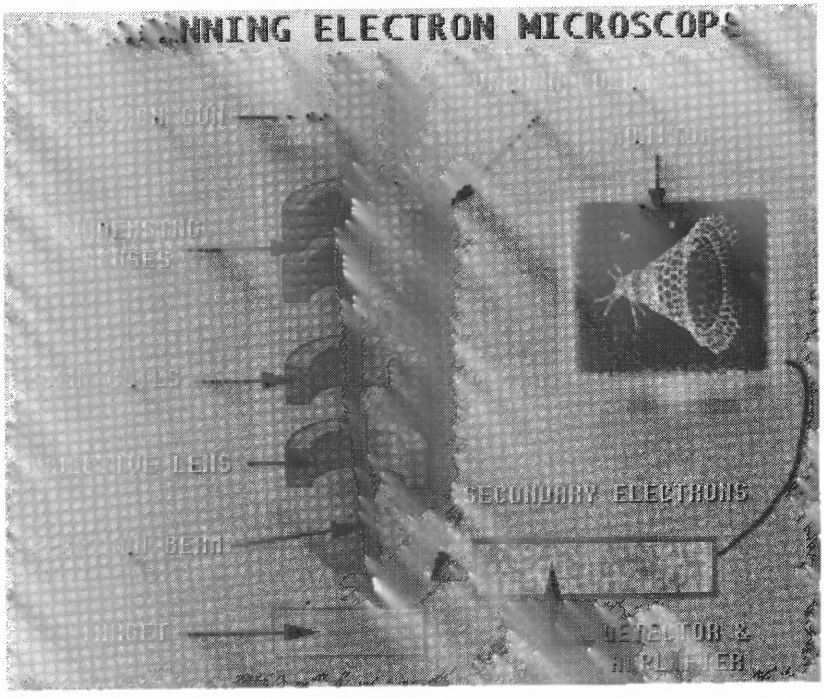


Figure 3.2 SEM principle. [34]

The SEM pictures of sample PL4-p, CO2-p, CO3-p was taken by FE-SEM LEO-1530VT model at an accelerated voltage of 5 kV and working distance of 6mm.

# CHAPTER 4

# RESULTS AND DISCUSSION

## 4.1 Characterization of Deposited Carbon Films

### 4.1.1 Raman Spectroscopy Results

For all the samples deposited in this project, no Raman spectrum peaks related to anhydride groups of PTCDA such as 1780, 1300 and 1000cm$^{-1}$ are detected. All five samples CO1-p to CO5-p show a peak around 1280 cm$^{-1}$ that is related to PPN structure [22]. For samples prepared by CVD in the system of Figure 2.1, CL5-p and CL7-p have this peak and for samples prepared by PECVD in the same system, PL4-p and PL5-p/Al have this peak.

Raman spectra of samples CO1-p, CO2-p, CO3-p, CO4-p, CO5-p, as shown in Figure 4.1 and Figure 4.2, have PPN characteristic peak, indicating that the temperature around 500-580°C does not decompose the aromatic rings of PTCDA but causes the anhydride groups to be cleaved. Thus PPN can be easily synthesized by CVD under this relatively low temperature.

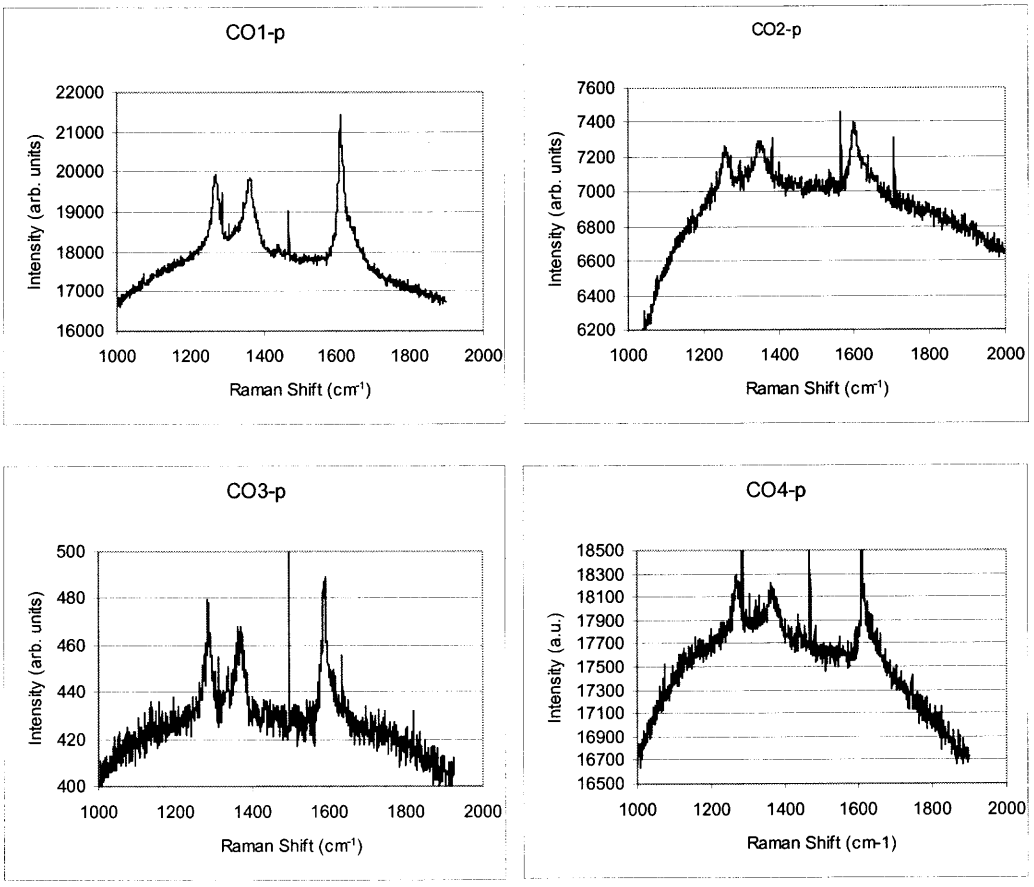


Figure 4.1 Raman spectra of samples CO1-p, CO2-p, CO3-p and CO4-p.

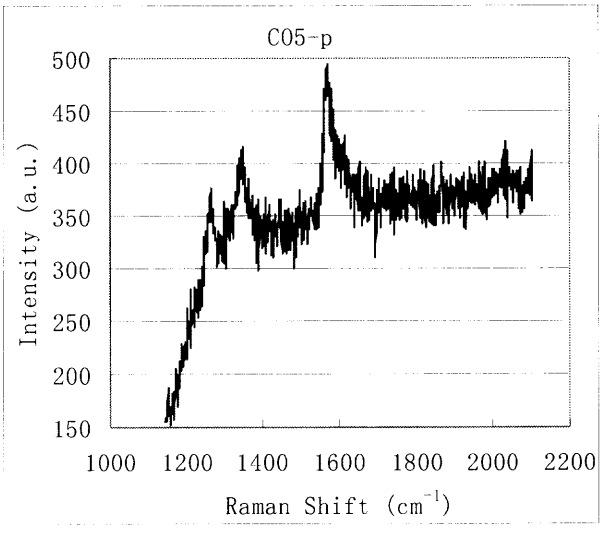


Figure 4.2 Raman spectrum of sample CO5-p (with the courtesy of Prof. Zafar. Iqbal).

Among those samples, CO3-p has the strongest 1280cm$^{-1}$ peak. Sample CO3-p was prepared at the temperature 510°C for PTCDA and 380°C for substrate in atmosphere pressure.

Peaks of CO1-p and CO2-p are broader and smaller than that of CO3-p, and sample CL1 (~400°C for PTCDA and 300°C for substrate) almost yield no deposit. It is inferred that lower temperature than that for CO1 (500°C for PTCDA and 355°C for substrate) would lead to low yield or a failure to undergo synthesis. None of these spectra, however, have peaks related to anhydride groups of PTCDA around 1000, 1300 and 1780cm$^{-1}$, indicating that the films do not contain PTCDA.

Sample CO5-p (Figure 4.2) has the highest 1580cm$^{-1}$ peak (G bond) to 1350cm$^{-1}$ peak (D bond) ratio, indicating a higher degree of crystalline order [28].

For samples CL4, CL6, CL8, CL9, CL10 and CL12 the Raman spectra show no PPN peak, though the operating temperature range was near to that of samples CO1-p to CO5-p discussed above. The reason could be a lower temperature or an uneven temperature distribution of vapor in the tube of system Figure 2.1. It was observed that during deposition there was quite a bit of red deposit on inner wall of the tube (PTCDA is red). So for these samples, the vapor temperature was likely below the substrate temperature displayed by the thermocouple. Raman spectra of samples CL2, CL4 and CL6, shown in Figure 4.3 and 4.4, that of samples CL8, CL9, CL10 and CL12 are almost same as CL6.

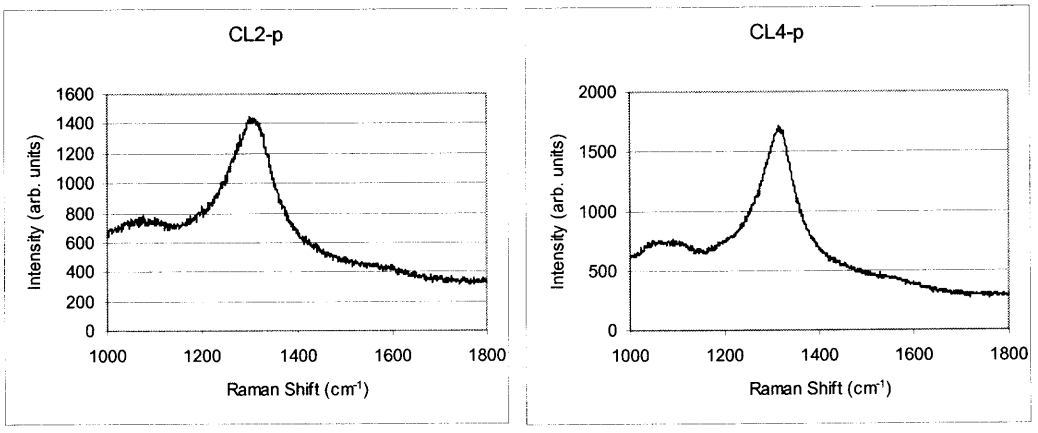


Figure 4.3 Raman spectra of samples CL2-p and CL4-p.

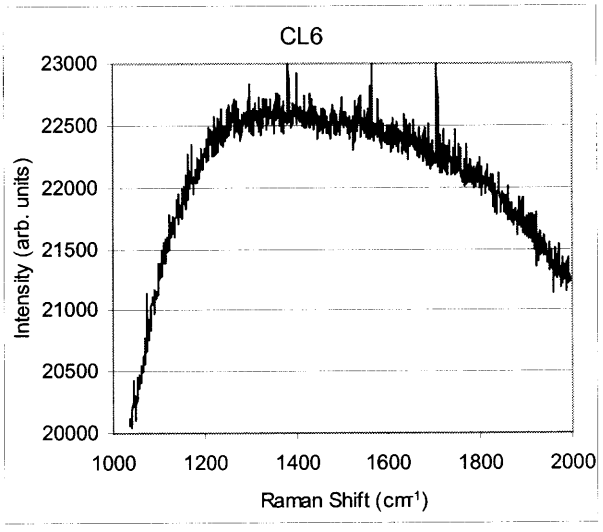


Figure 4.4 Raman spectrum of sample CL6.

In order to check the effects of the vapor temperature, a copper tube surrounding the substrate and heated by the halogen lamps was used during deposition (sample CL7-p). It was expected that in this configuration the gas near the substrate and the substrate itself will have the same temperature. And to check if illumination has destructive effect on PPN formation, sample CL5-p was deposited by illuminating

directly the surface of the deposited film, rather than the back side of the substrate, with other conditions the same as for sample CL6. Raman spectra of sample CL7-p and CL5-p are shown in Figure 4.5.

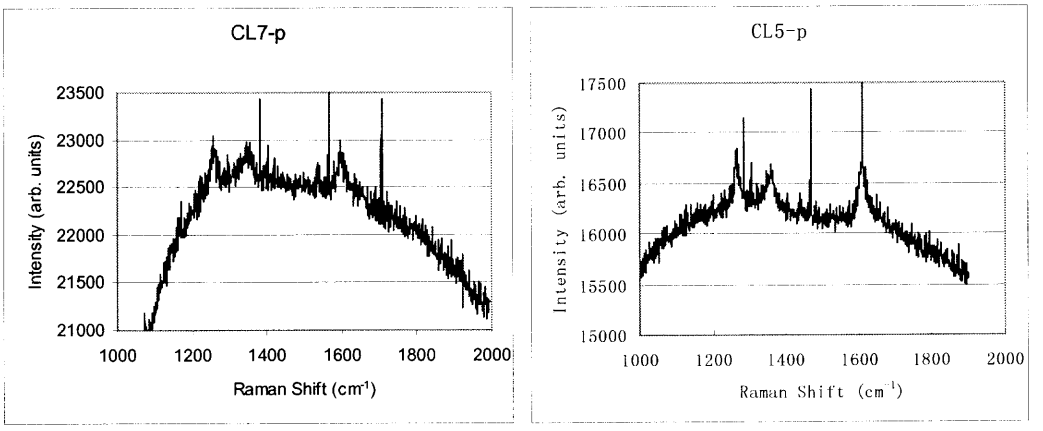


Figure 4.5 Raman spectra of samples CL7-p and CL5-p.

Samples CL7-p and CL4, CL5-p and CL6 were deposited in same system and at same pyrolysis and deposition temperatures, respectively. Raman spectra of CL7-p and CL5-p apparently have characteristic PPN peak around 1280 $cm^{-1}$. So vapor temperature is crucial to synthesis of PPN and light is not detrimental to this process. It can be assumed that the illumination of the film surface, rather than the back side of the substrate, also heats more effectively the gas near the growing film.

In spectra of samples PL3/Al (Al substrate very close to the source of PTCDA), and samples PL6, PL7 and PL9 (Figure 4.6), only two peaks, corresponding to the disordered (D) peak (1350$cm^{-1}$) and graphitic (G) peak (around 1600$cm^{-1}$) are evident. This indicates that the films are of amorphous graphite since a higher intensity of

G-band indicates the higher degree of crystallinity/graphitization. These four samples were prepared by PECVD.

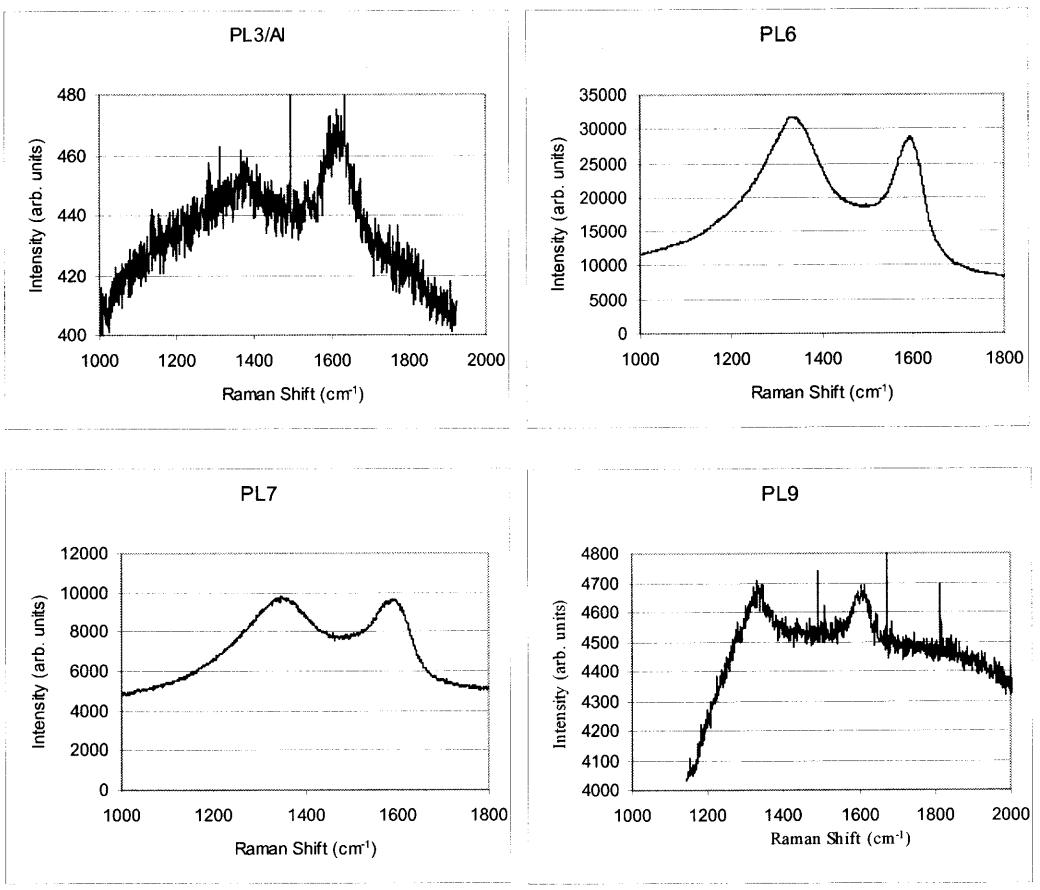


Figure 4.6 Raman spectra of samples PL3/Al, PL6, PL7, PL9.

Relative intensity ratio of D and G peaks ($I_D/I_G$) is a measure of the amount of disorder in the crystallinity [35], For PL3/Al , $I_D/I_G$ is low.

Meenakshi and Subramanyam [29] found that graphitic order (*G*-peak width and position) of carbon film, obtained by pyrolysis of an anhydride precursor, tetra chloro phthalic anhydride, TCPA ($C_8C_{l4}O_3$), is not affected by variation in pyrolysis temperature (700-900°), based on the results of XRD. The significant reduction in the

width of the *D* peak (characterizes disorder) in films deposited at higher temperature (900°C) indicates the reduction of bond-angle disorder (associated with the transition to metallic state). This is congruous with result of samples PL3/Al, PL6, PL7 and PL9 that were obtained by PECVD.

Because relatively high DC discharge power tends to destroy the original condensed aromatic rings in the source monomer (PTCDA), the polymer product under such condition is only an amorphous film. There should be optimum DC power to prepare the polymerized film. Relative low DC power used in the deposition of samples PL4-p and PL5-p/Al seems to confirm this.

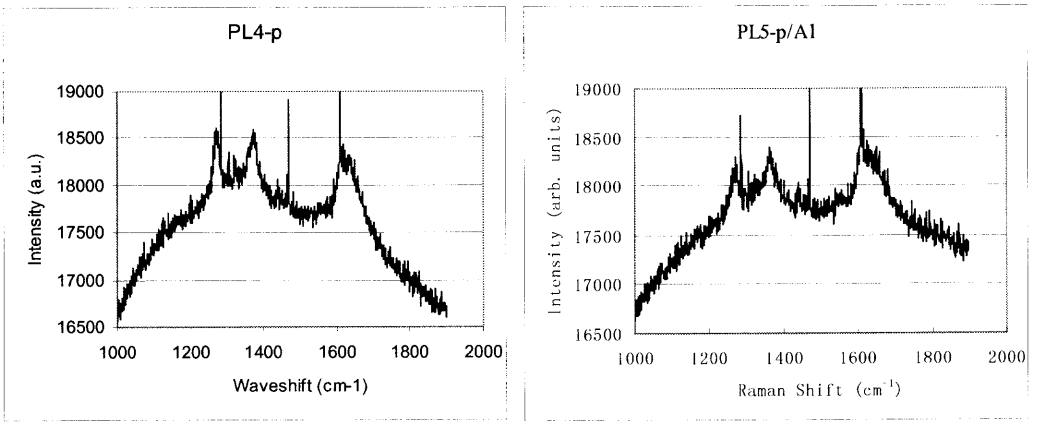


Figure 4.7 Raman spectrum of samples PL4-p and PL5-p/Al.

Raman spectra of samples PL4-p and PL5-p/Al film show a peak of PPN at 1280 $cm^{-1}$ as well as those at 1580 and 1350 $cm^{-1}$, the characteristic of the amorphous carbon materials. So the plasma with relatively weak DC power basically only cleaves the side group but does not destroy the condensed aromatic rings of PTCDA.

The spectrum of PL4-p is different from that of CO3-p in peak intensity, this along with differences between SEM pictures of PL4-p and CO3-p (Figure 4.11 and Figure 4.13) signifying the development of cross-linked structure in film PL4-p.

Sample PL3 was deposited under similar conditions as PL4-p, except for the lower pressure (0.8 torr for PL4-p and 0.19 torr for PL3), but PL3 barely contains PPN structure (Figure 4.8). The difference may be caused by a higher ion energy with lower pressure for PL3, since $E_{ion} \propto (1/P^m)$; $0 \leq m \leq 1$.

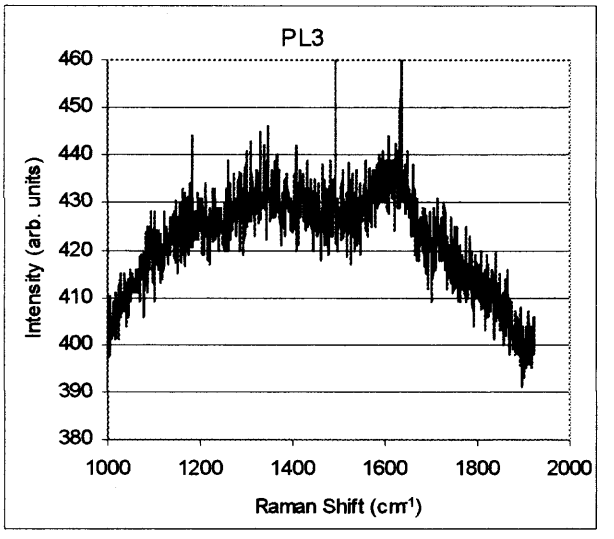


Figure 4.8 Raman spectrum of sample PL3.

It's worthy of note that some samples have a weak 1200 $cm^{-1}$ peak, which provides evidence for the presence of "polymeric" domains. Presence of this "polymeric domains" containing chains of carbon atoms with single and double bond alternation (-C=C-), could give rise to anomalous features [29].

### 4.1.2 XRD Results

It was found that the X-ray diffraction pattern had contribution from the substrate (around 45, 82, 65°), as the thickness of the films are only about 1-2 μm [22] and the films density is only about 1.7g/cm$^3$ [32].

Low-angle features are commonly observed in polymer-like amorphous carbon films [30] [33]. XRD analysis of Sample PL4-p and CO3-p that partially contain PPN structure yield no diffraction lines (except that of Fe substrate).

According to reference [30] the XRD pattern of the carbon films prepared by pyrolysis of anhydride such as PTCDA and maleic anhydride has a broad amorphous hump around 22°-23°. Sample CL12 was prepared by heating PTCDA to 510°C and substrate to relative high substrate temperature of 500°C for 4 hours, the XRD data of sample CL12 exhibits more features than what is found in disordered carbon films. The film was found to be polycrystalline, as shown in Figure 4.9, the *d* ranges from ~3.70 Å to ~1.17 Å or less. There could be the crystal of graphite (24, 44.6, 54°), other carbons (including lignite and chaoite) (30, 33, 40.8, 42, 43, 49.3, 62.5, 64°), diamond (44.6, 75°), and iron carbide ($Fe_2C$, $Fe_3C$, $Fe_{20}C_9$) (35.6, 40.8, 54, 62.4, 89°). The strong peaks characteristic of PTCDA powder diffraction 2θ scans [36] do not appear here.

The peak around 24°, in XRD pattern of sample CL12, points to a layered structure though it occurs at a lower angle compared to that in graphite. According to the Brag's formula, $d=\lambda/(2\sin\theta)$, the interlayer distance is ~3.64Å, that is considerably higher than that of graphite (3.355Å) [30]. This may be due to the reduction in packing

efficiency caused by disorder. The misalignment of graphite-like planes increases the separation between them, causing the peak to shift to lower angles.

Figure 4.9 shows a bump at 9°C. Murthy *et al.* [36] reported a low-angle peak (9° peak) corresponding to the plane spacing of 10 Å observed in x-ray diffraction scans of partially pyrolyzed PTCDA at 530°C. Based on simulations of structure and diffraction patterns using molecular dynamic calculations, they think this peak is attributed to the distance between columns of rotationally disordered, partially pyrolyzed PTCDA molecules in a discotic phase, which is a precursor to graphitic structures.

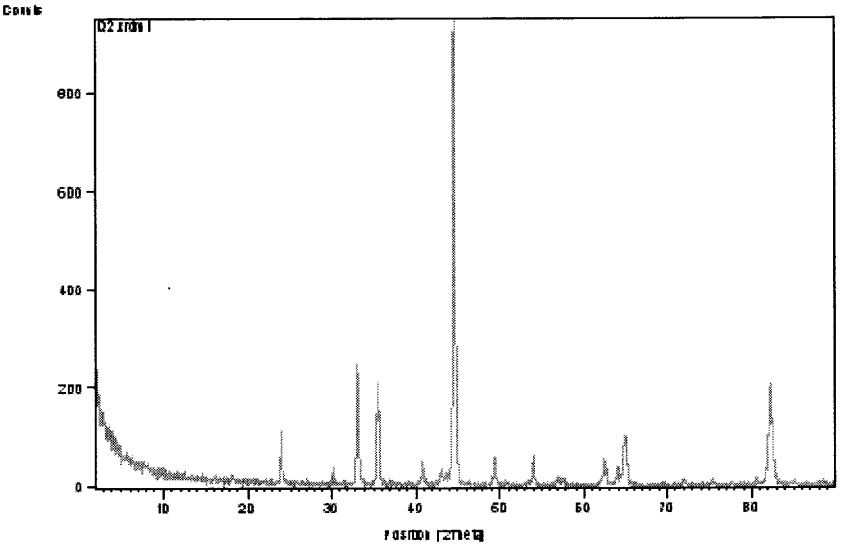


Figure 4.9 XRD pattern of sample CL12.

XRD patterns of sample PL4-p (Figure 4.10) and sample CO3-p are almost the same. Figure 4.10 indicates the crystallinity of the deposited PPN film was low. There is no broad peak around d=0.34 nm corresponding to the d value of (011)

planes of phase II of PPN [22].

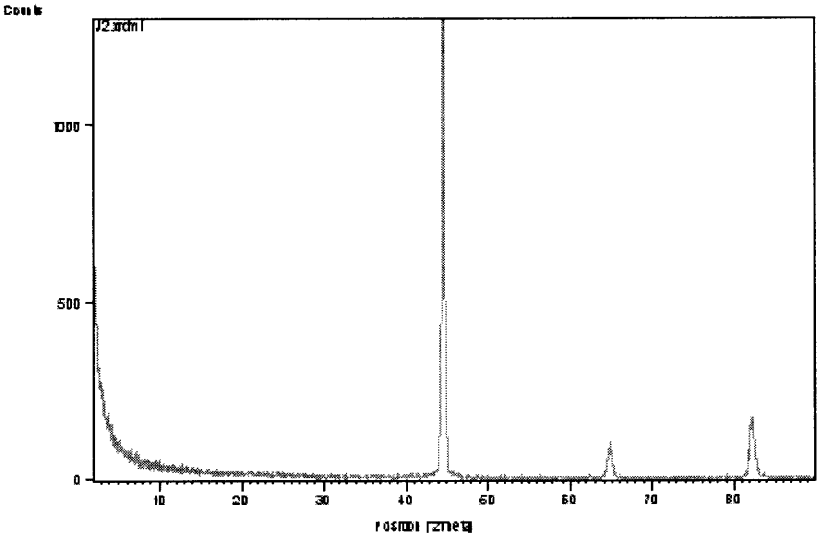


Figure 4.10 XRD pattern of sample PL4-p.

### 4.1.3 SEM Results

SEM images of different magnification were detected for three samples. The pictures of sample PL4-p and CO2-p are alike that of samples in reference [14] with cross-linked structures and entangled long fibrils respectively. Sample CO3-p has 1 μm fracture chains of diameter about 100 nm and length 0.5 - 1 μm.

SEM figures show a wide variety of surface morphology at different locations on the films CO2-p and CO3-p. In contrast, SEM pictures of sample PL4-p, shown in Figure 4.11, reveal a relatively smooth surface with uniform cross-linked structures. Forrest et al. [32] prepared films from ion beam irradiated PTCDA, which also do not have linked long one-dimensional chains. The same structure appeared in Reference [14].

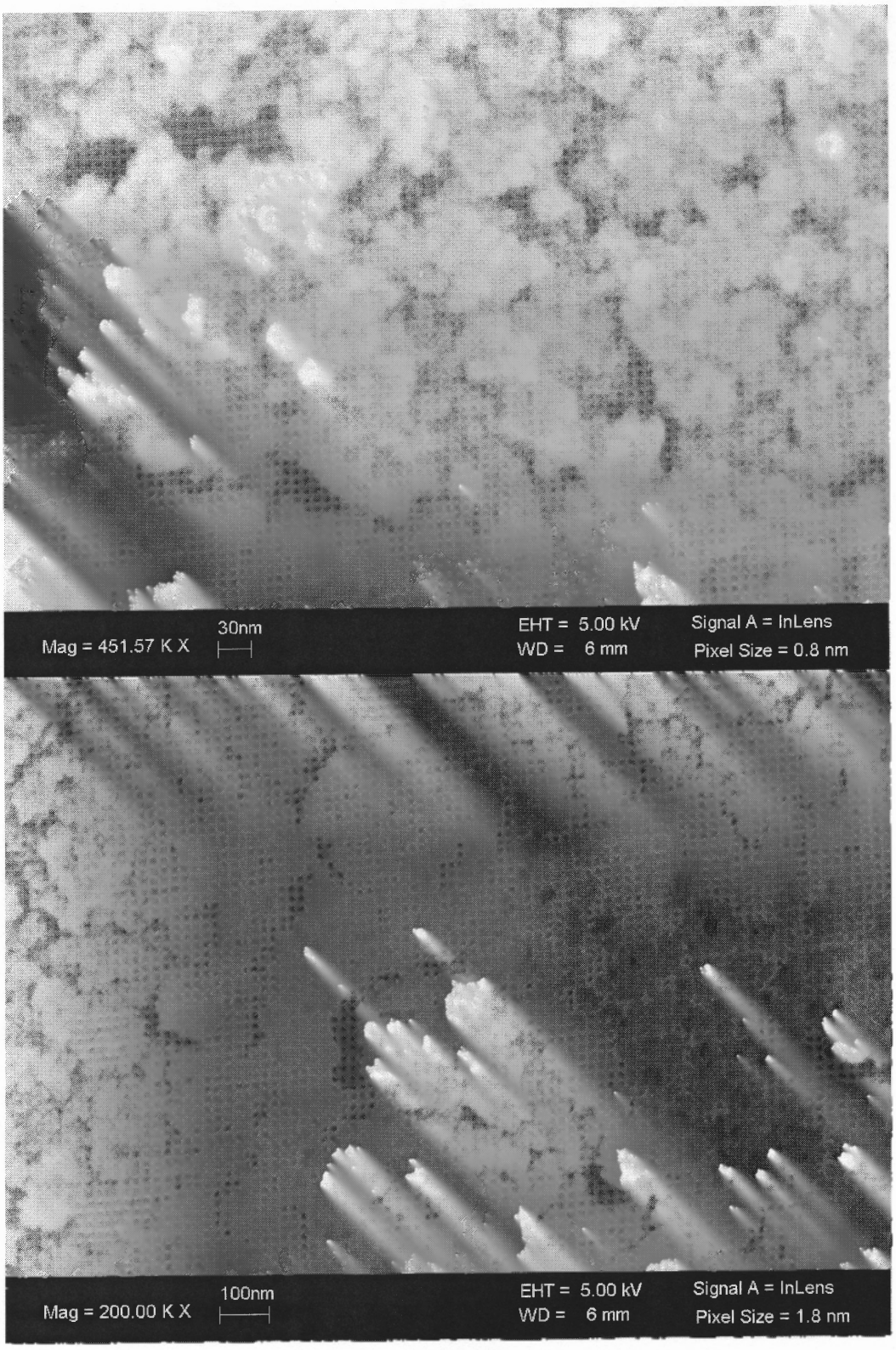


Figure 4.11 SEM pictures of sample PL4-p.

SEM pictures of samples CO2-p and CO3-p (Figure 4.12 and 4.13), along with Raman spectra and XRD results, confirms that samples CO2-p and CO3-p are homogeneous organic thin film involving the 1-D-graphite skeletons of PPN. Sample CO2-p consists of entangled long fibre with diameter around 1 μm. Sample CO3-p has more gracile fiber than that of CO2-p: diameter around 100 nm and length around 0.5-1.0 μm.

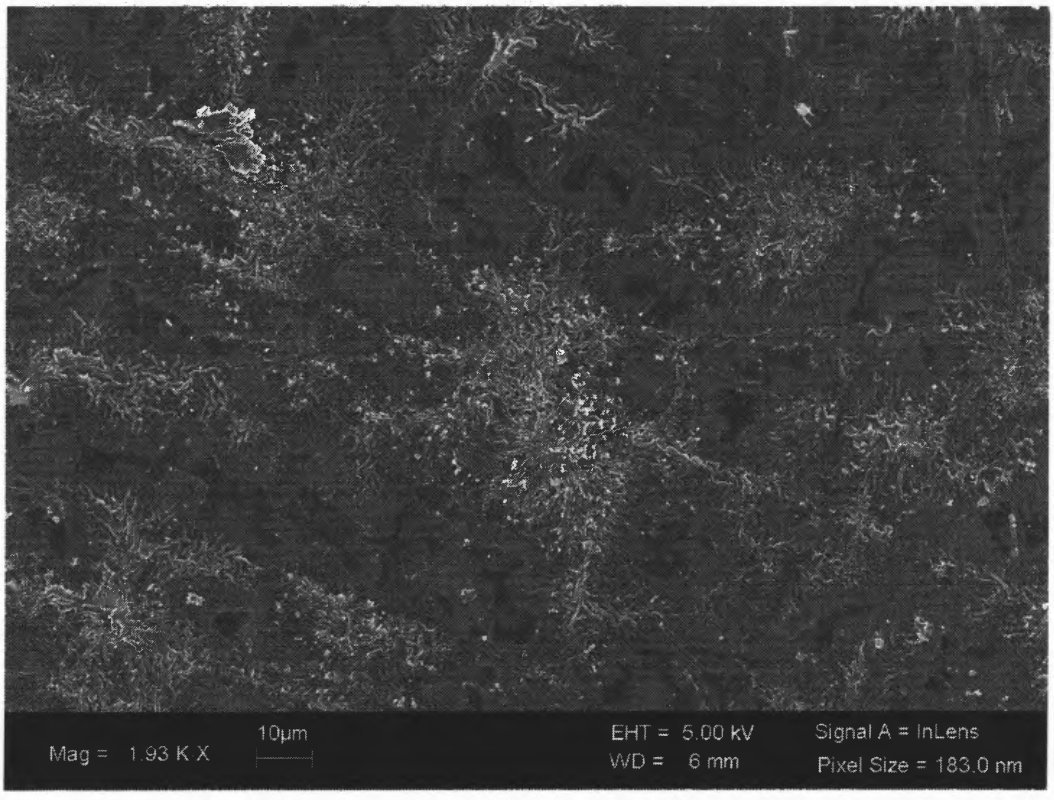


Figure 4.12 SEM pictures of sample CO2-p.

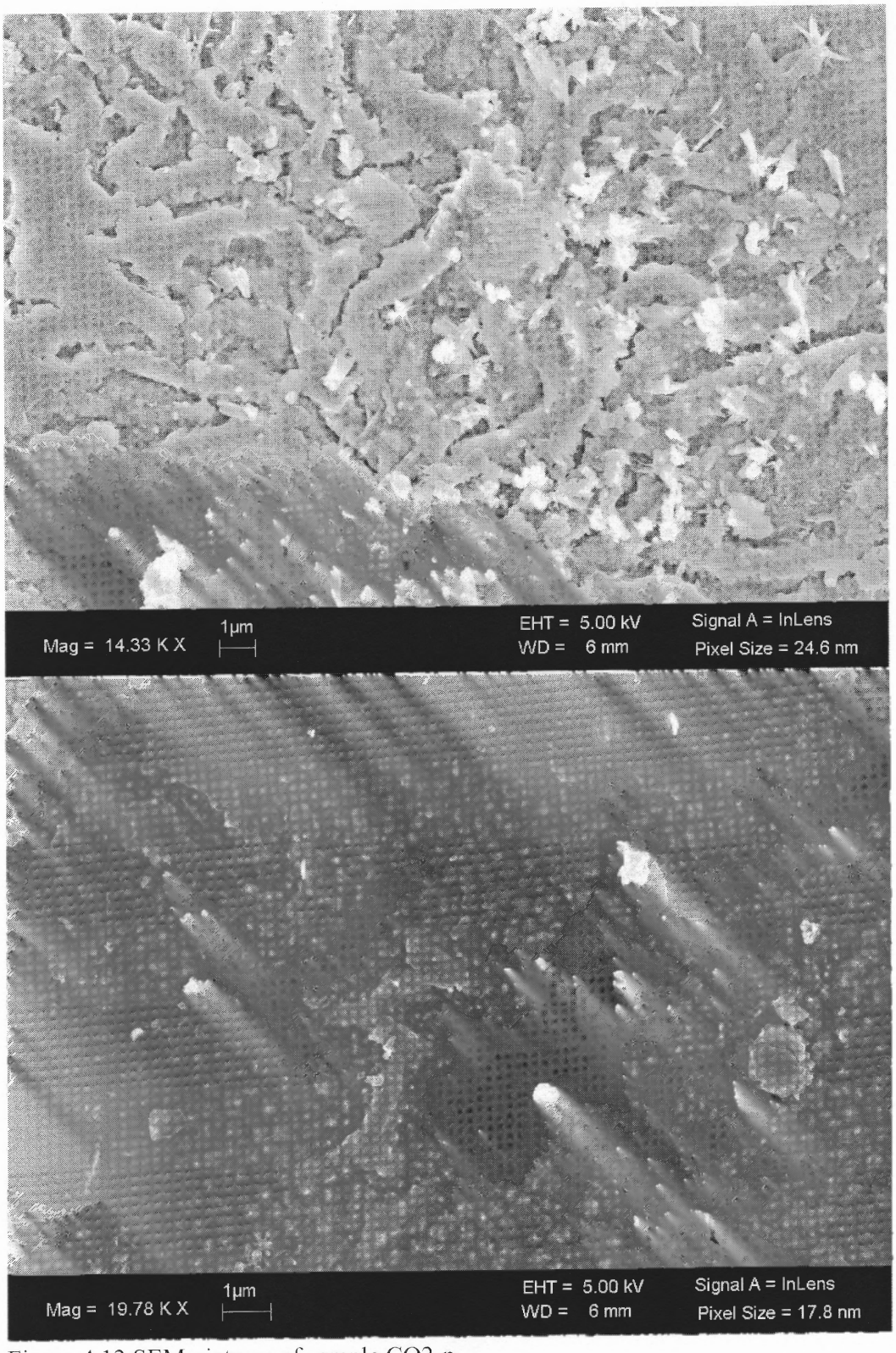


Figure 4.12 SEM pictures of sample CO2-p.
(Continued)

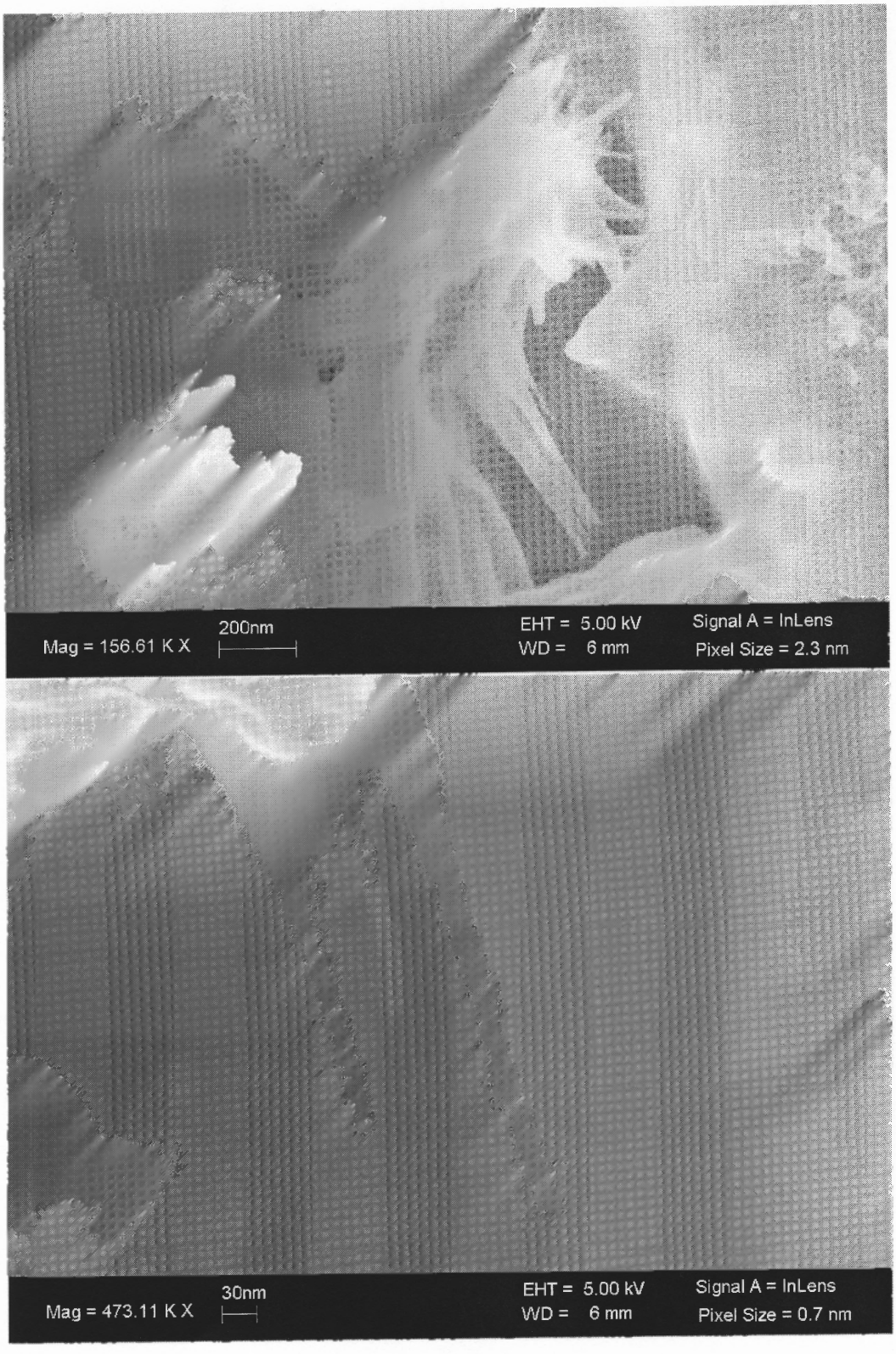


Figure 4.12 SEM pictures of sample CO2-p.
(Continued)

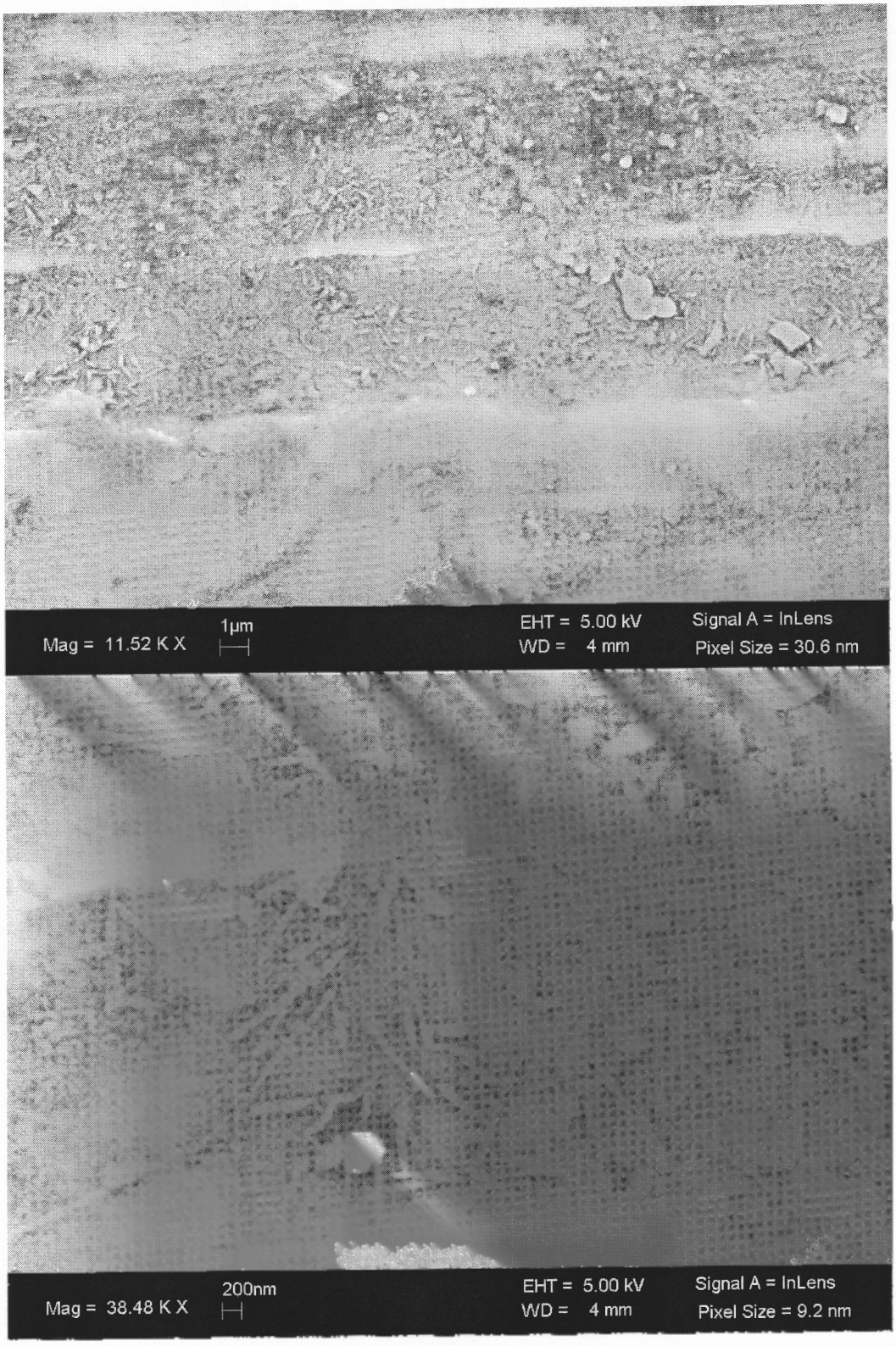


Figure 4.13 SEM picture of sample CO3-p

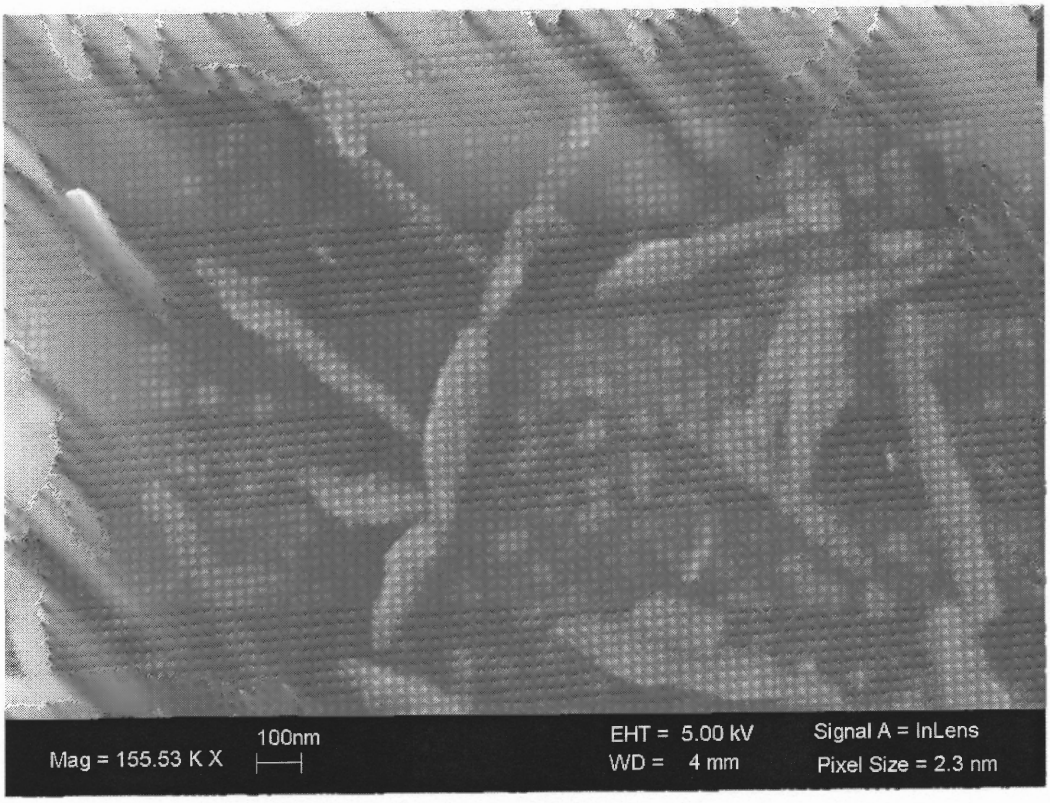


Figure 4.13 SEM picture of sample CO3-p
(Continued)

Yoshimura et al. [24] have shown a transmission electron microscopy (TEM) picture of the PPN fibers annealed at 2800°C, which reveals the graphitized PPN consisting of one-dimensional chains of graphite oriented normal to the direction of the fiber axis. This result along with a SAD pattern of the PPN fiber synthesized at 530°C, confirms that the intermediate perylene molecules are linked to form the PPN chain in the direction normal to the fiber axis.

## 4.2 Discussion of the Deposition Process Parameters on the Characteristics of Carbon Films

The structure and properties of the films products from PTCDA by thermal CVD and

PECVD depend on the deposition conditions of temperature, pressure, plasma discharge conditions, etc. These parameters were varied to examine the appropriate conditions for preparation of the films with desirable characteristics.

### 4.2.1 Influence of Pressure

The reaction is thought to proceed in the vapor phase [11]. The vapor-phase polymerization proceeded by a radical reaction of perlene-tetraradical (Ⅳ) and PDCA-diradical (Ⅴ) (see Figure 1.10). So the vapor partial pressure of above radicals has significant influence on deposition.

Pressure and power are expected to be primary parameters concerning the film properties when PECVD method is used. Samples PL3 and PL4-p, PL5-p/Al were prepared in the same range of DC power (Ic~ 0.02A, Vc~ 1000V), but pressure for PL3 was lower than that of PL4-p and PL5-p/Al. Decreasing deposition pressure leads to the increase of the density and energy of electrons in the plasma. [9], so higher energy for PL3 interdicted the formation of PPN, while as the pressure increases to a certain level, the ion energy becomes so low that it cannot overcome existing activation barriers to adsorption and the gas phase polymerization dominates [9].

The reaction gas was a mixture of carrier Ar gas and sublimed vapor of PTCDA. In PECVD process, there is a competition between deposition and sputtering, at the PTCDA low vapor pressure (when sublimation temperature is low), the flux of radicals in the plasma is much smaller compared with the $Ar^+$ flux. The etching effects of films by the sputtering of Ar ions are dominant, and no films can be deposited.

With the increase of PTCDA vapor pressure, the sputtering rate decreased and the deposition process starts to play a role and dominates in film growth.

### 4.2.2 Influence of Temperature

Pyrolysis of organic compounds under suitable conditions lead to graphite-like materials and typically their properties are strongly influenced by the starting precursor and pyrolysis temperature. Condensation of polyfunctional monomers followed by heat treatment at higher temperatures is expected to yield ladder-type polyconjugated systems with a highly conjugated and rigid polymer backbone [24]. The electrical conductivity in general increases with increasing the heat treatment temperature, which corresponds to carbonization or development of extended aromatic structures [24].The results from conductivity measurements [46] [29]were indicative of a possible transition from a metallic to semiconducting behavior with pyrolysis temperature. Electrical conductivity measurements undertaken on carbon films prepared from PTCDA suggested the possibility of a metal-insulator transition as a function of pyrolysis temperature [30].

The substrate temperature is also an essential parameter for the deposition. In this project, before some modifications to the system shown in Figure 2.1, the samples (such as CL4, CL6) have not contained PPN structure, after modifications (CL7-p was surrounded by a copper tube, CL5-p was illuminated directly on the surface) the synthesized films contain PPN. This indicates that the gas temperature neat the growing film surface, and not only the substrate temperature is important.

With increasing substrate temperature (in this project CVD from 300 to 400°C, PECVD from 200 to 350°C) π-conjugated system is developed by effective recombination of radicals, in favor of synthesis of PPN.

### 4.2.3 Influence of Plasma Condition

In PECVD, the structure and properties of the films is sensitive to plasma condition. The energy of Ar ions is low at low DC discharge power, the sputtering effect of Ar ions can be neglected, polymer-like films with a fraction of PPN structure can be deposited. High DC discharge power destroys the aromatic rings. To prepare PPN films from PTCDA, low discharge power (several watts) combine with relative low sublime temperature and substrate temperature is preferred.

### 4.2.4 Other Influence Factors

**Influence of Air**

PPN is expected to be stable against oxygen because it has a structure of fused aromatic rings. [37] It's reported [14] that conductivity of plasma-polymerizated PPN films, using PTCDA as precursor, decreased upon exposure to air, probably owing to compensation effect to the conduction carriers or scavenging the dangling bonds to impede the conduction paths by oxygen. Raman spectrum peaks of Sample PL9 (very thin film) disappeared after two months. It is assumed that the contact with air caused the change.

**Influence of Light**

PAHs (PTCDA is PAH) can undergo photodecomposition when exposed to ultraviolet light from solar radiation [38].

Schmidt et al. [39] found that electron beam exposed regions of PTCDA display pronounced photoconductivity. The resistivity was observed to decrease by an order of magnitude with moderate incandescent illumination levels.

Yudasaka et al. [37]found that in the pulsed laser deposition using a target of PTCDA the surface of the target was pitted by the laser light, the Raman spectrum of this irradiated zone was not that of PPN but had the long tail of luminescence characteristic of PTCDA. Therefore, during the pulsed laser deposition, the laser light is considered to evaporate and decompose PTCDA but not produce PPN on the target.

Sample PL5-p/Al has been covered on both sides, the film on the side exposed to heating light directly has characteristic PPN peak in Raman spectrum, however the film on the other side has not such peak, under deposition condition of PL5-p/Al, light could help in increasing the gas and the substrate surface temperature or help cleave side groups of PTCDA and conjoin PPN chain. It's currently not easy to discuss the rationalization of such a parameter dependency owing to the difficulty in analyses of the two parameters, light and surface temperature, separately in this system (Figure 2.1).

**Substrate**

Different substrates (stainless steel, aluminum, quartz and silicon) were put beside

some samples during the deposition. No significant deposits were found on quartz and silicon substrates and neither on the Al substrates in CVD process. This can be attributed to catalysis effects of Fe for the formation of PPN [22] [40]. Almost all stainless steel substrate were covered with good uniform films that were hard to scrape off. They are CO4-p/stainless, CO2-p/stainless and CO3-p/stainless etc. The comparison of Raman spectra of films on gun steel substrate and on stainless steel in Figure 4.14 shows that the stainless steel substrate promotes synthesis of PPN better than gun steel substrate especially at lower pyrolysis temperature.

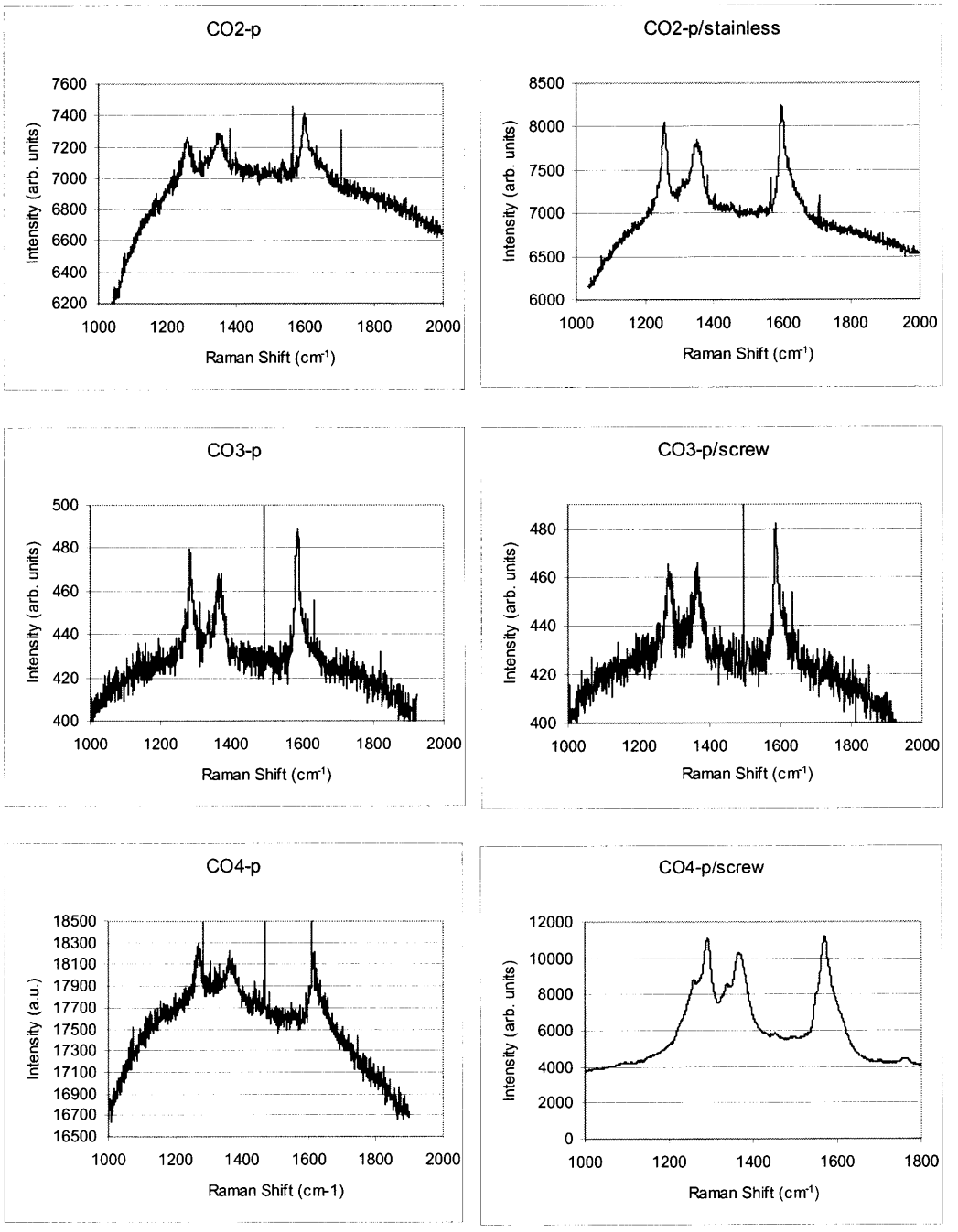


Figure 4.14 Comparison of Raman spectra of films on different substrate.

Sample CO3-p/stainless has apparent different surface morphology from sample. CO3-p (see Figure 4.15 and Figure 4.13), sample CO3-p/stainless looks like dense smooth shiny black film, while CO3-p dull black. Raman spectrum of sample

CO3-p/stainless has less intensity PPN peak than that of CO3-p and CO3-p/stainless.

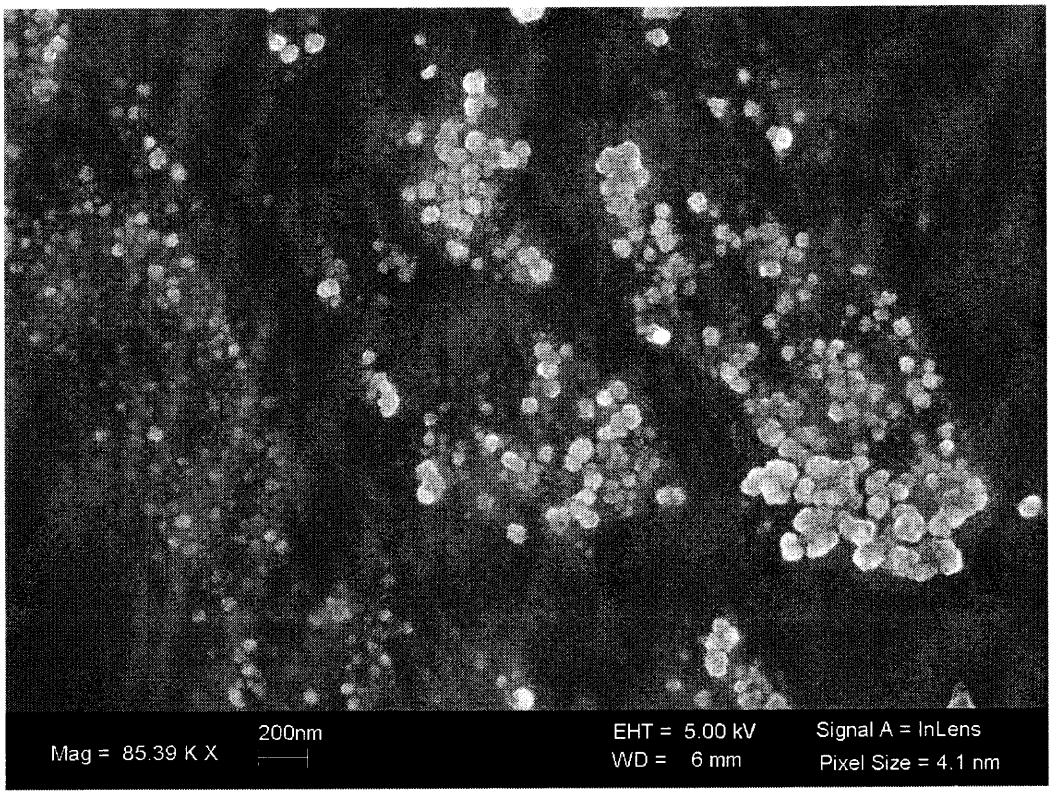


Figure 4.15 SEM picture of sample CO3-p/stainless.

The chemical composition of gun steel and stainless steel is listed in APPENDIX C. Stainless steel contains less nonmetal elements and more chromium, nickel, manganese than gun steel. This could be the reason for better coating and more distinct PPN peak in Raman spectra.

### 4.3 Optimum Deposition Parameters for PPN Films

In this project, the films containing PPN structure are samples CO1-p, CO2-p, CO3-p, CO4-p, CO5-p, CL5-p and CL7-p deposited by CVD, and samples PL4-p, PL5-p/Al

deposited by PECVD. The deposition parameters of CO3-p are the best for synthesis of PPN by CVD.

The best CVD deposition conditions are 510°C for PTCDA source and 380°C for substrate (Fe, Ni, Co) in 1 atm pressure. The best PECVD depostition conditions are ~350°C for PTCDA and ~350°C for substrate with low DC power of several watts at ~1 torr pressure. We can infer that under these conditions formation of PPN occurred by removal of CO and $CO_2$ from the dianhydride groups. The peri-free radicals formed then polymerize yielding the new material, PPN.

PL4-p and PL5-p/Al has uniform structure and smooth surface and much higher deposition rate. They demonstrate that PECVD has potential for deposition of high quality PPN films, even without iron as catalyst.

### 4.4 Comparison between CVD and PECVD

It's easy to prepare carbon films containing PPN chain by CVD method. The important parameters that affect formation and properties of film containing PPN are sublimation temperature, substrate temperature (surface temperature) and moderate inert gas flow at atmosphere pressure. Difficulty in obtaining high growth rate in CVD method requires long deposition times (hours) and prevents obtaining thick films.

In PECVD process, it's assumed that perylene tetraradicals radicals from the plasma adsorb at the surface in a physisorbed state, the coverage of the surface depends on the surface temperature, pressure, and plasma condition. With plasma's

enhancement, the required sublimation temperature and substrate temperature are decreased significantly, and the presence of high energy free electrons and ions aims in formation of uniform film with high deposition rate. The plasma energy, however, can not be too high because the aromatic rings of the precursors may be destroyed by molecular scission and energetic ions can sputter the films as fast as it grows.

# CHAPTER 5

# CONCLUSION

A study was carried out on the synthesis and characterization of carbon films containing PPN, a representative one-dimensional graphitic polymer. Depositions by CVD and PECVD using PTCDA as a precursor were made primarily on steel substrates. The process parameters were systematically varied and their effects on the films properties were investigated. The films were characterized by Raman spectroscopy, XRD and SEM and the results were compared to information in the recent literature.

The structures and properties of the deposited carbon films with PPN are related to the deposition conditions which control the mechanisms of the carbon film formation. The polymerization reaction involves the thermolysis of the carboxylic groups with elimination of carbon dioxide and monoxide gases and coupling of perylene tetraradicals. Pyrolysis induce polyconjugated systems with planar ladder-type chains or extended aromatic rings. With this structure PPN is expected to have high environmental stability and high conductivity comparable with graphite. [24]

The most promising deposition conditions were obtained by setting the following parameters:

1. CVD: 510°C for source material (PTCDA), 380°C for substrate (Fe, Ni, Co) in 1 atm pressure in Ar gas.
2. PECVD: ~350°C for source material (PTCDA), ~350°C for substrate, in Ar gas at ~1torr pressure, DC power of several watts.

For these conditions, the films were found to have PPN characteristic peak around 1280 $cm^{-1}$ in Raman spectra.

The material has potential industrial applications because of its durability, suitability for use as anticorrosive coating, and good electrical conductivity. The CVD process is well controlled but it has low deposition rate. PECVD promises higher deposition rate at lower temperature.

Further studies are suggested with introducing a bias voltage on the substrate in PECVD and with adjusting the partial pressure of PTCDA vapor in CVD.

## APPENDIX A

## PROPERTIES OF PERYLENE AND NAPHTHALENE

**Perylene:**

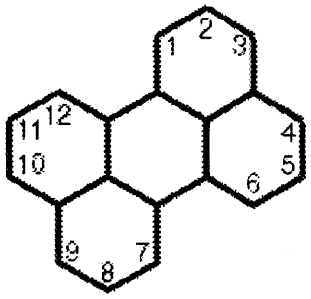


An organic molecule consisting of 20 carbon atoms and 12 hydrogen atoms arranged as five benzene-like rings connected to each other in a plane, has shown promise as a material for organic versions of field-effect transistors (FETs).
$C_{20}H_{12}$
Appearance: brown solid
Melting point: 277 - 279 °C
Boiling point: 497 °C [48]
Stable. Incompatible with strong oxidizing agents. Combustible. [45]

**Naphthalene:**

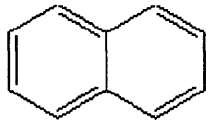

Naphthalene is formed by the fusion of two benzene molecules and has $10\pi$ electrons. Naphthalene is a white, crystalline solid, with a characteristic benzenoid electronic spectrum.
$C_{10}H_8$
Melting point: 81 °C
Boiling point: 218 °C [48]

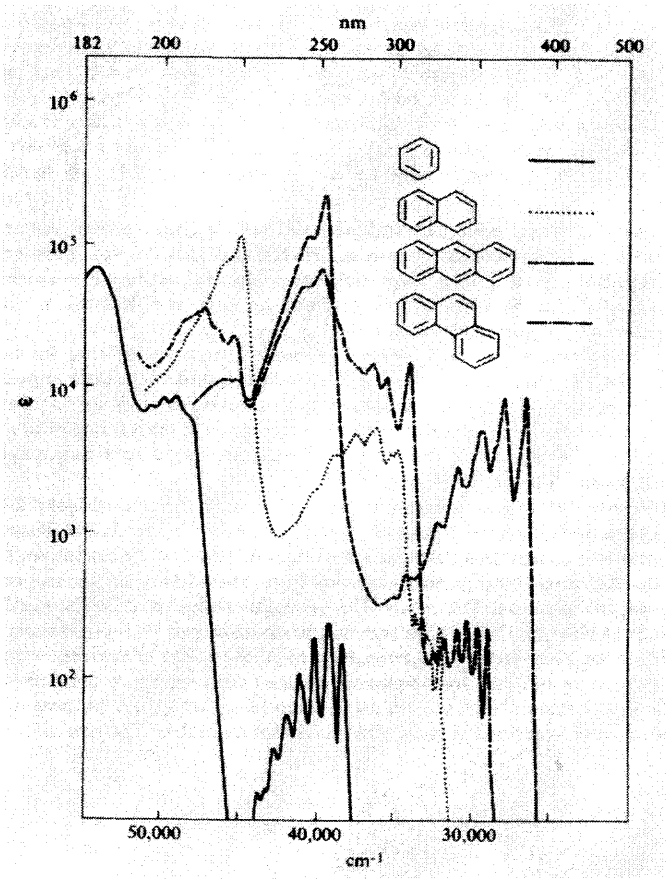


Figure A.1 Electronic spectra of benzene, naphthalene, anthracene, and phenanthrene in hexane. [44]

It is diatropic and undergoes electrophilic substitution. The physical and chemical properties of naphthalene are thus those expected for a classic aromatic system. In the Huckel model, the σ framework is fixed and each of the 10 carbon atoms supplies one $2p$ atomic orbital to the π system. [44]

# APPENDIX B

## SOME DATA ON 3,4,9,10-PERYLENE TETRACARBOXYLIC DIANHYDRIDE (PTCDA)

Sublimation temperature of 3,4,9,10-perylene tetracarboxylic dianhydride (PTCDA) is 360°C.

Raman spectrum peaks at 1750 $cm^{-1}$, 1780 $cm^{-1}$, 1300 $cm^{-1}$ and 1020 $cm^{-1}$ related to the side groups of PTCDA monomers and a peak at 1600 $cm^{-1}$ related to condensed aromatic ring of perylene skeleton in the PTCDA film. [43]

IR spectra of PTCDA has absorption bands at 1770$cm^{-1}$ ($\nu_{C=O}$), 1760 $cm^{-1}$ ($\nu_{C=O}$), 1600 $cm^{-1}$ (aromatic $\nu_{C=C}$), 1400 $cm^{-1}$ (aromatic $\delta_{C-H}$ in plane), 1300 $cm^{-1}$ ($\nu_{C-O-C}$ of anhydride) and 1020 $cm^{-1}$ (dianhydride stretch). The absorption bands at 860,800 and 750 $cm^{-1}$ are assigned to aromatic $\delta_{C-H}$ vibrations. The peak around 3100 $cm^{-1}$ is due to aromatic C-H stretch. [22]

PTCDA has been used as functional materials in such fields as organic photoconductors, solar energy conversion, liquid crystal displays, and photoelectron molecular devices [47].

## APPENDIX C

## CHEMICAL COMPOSITION OF GUN STEEL AND STAINLESS STEEL

Table C.1 Chemical composition of gun steel and stainless steel.

| Element | Gun Steel [41] (wt.%) | 304 stainless steel [42] (wt.%) |
|---|---|---|
| Carbon | 0.37 | 0.07 |
| Manganese | 0.47 | 2.00 |
| Silicon | 0.02 | 1.00 |
| Chromium | 0.85 | 17~20 |
| Nickel | 3.17 | 8~10 |
| Molybdenum | 0.65 | -- |
| Phosphorus | 0.006 | 0.045 |
| Sulfur | 0.01 | 0.03 |

## REFERENCES


1. A. Sayeed, V. Meenakshi, S. V. Subramanyam, A. Cholli and S. Tripati, "Highly conducting amorphous phase of carbon", Chemistry for Sustainable Development 8 (2000) pp.55-58.

2. http://ie.jrc.cec.eu.int/htr-tn/ECS2002/Bourrat_570.pdf.

3. Helga Schultrich and Bernd Schultrich, "TEM simulation of nano-structured carbon films", EUREM 12, Brno, Czech Republic, July 9-14, 2000, p.247.

4. P. Delhaes, "Chemical vapor deposition and infiltration processes of carbon materials", Carbon 40 (2002) pp.641-657.

5. Philip L. walker, JR. Peter A. Thrower, "Chemistry and Physics of Carbon", Volume 11, Marcel Dekker, INC. New York, 1973, ISBN: 0069-3138.

6. Masatoshi Murashima, Dazuyoshi Tanaka and Tokio Yamabe, "Electrical Conductivity of Plasma-Polymerized Organic Thin Films: Influence of Plasma Polymerization Conditions and Surface Composition", Synthetic Metals, 33 (1989) pp.373-380.

7. http://selland.boisestate.edu/jjozwiak/rf/01_plasma.ppt.

8. Brian Chapman, "Glow discharge Processes", A wiley-interscience publication, John Wiley & Sons, 1980, ISBN 0-471-07828-X.

9. Y.H. Cheng, Y.P. Wu, J.G. Chen, X.L. Qiao, C.S. Xie, B.K. Tay, S.P. Lau, X. shi, "On the deposition mechanism of a-C:H films by plasma enhanced chemical vapor deposition", Surface and Coatings Technology 135 (2000) pp.27-33.

10. Zi Jun Hu, Klaus J. Huttinger, "Mechanisms of carbon deposition – a kinetic approach", Letters to the editor / Carbon 40 (2002) pp.624-628.

11. M. Murakami, "Morphology and polymerization mechanism of one-dimensional graphite polymer, poly-peri-naphthalene", Synthetic Metals, 18 (1987) pp.532-537.

12. Giese, Bernd, "Radicals in Organic Synthesis: Formation of Carbon-Carbon Bonds", Oxford [Oxfordshire]; New York: Pergamon Press, 1986, ISBN: 0080324932: 0080324940 (pbk).

13. Hisashi Kajiura, Houjin Huang, Shigemitsu Tsutsui, Yousuke Murakami, Mitsuaki Miyakoshi, "High-purity fibrous carbon deposit on the anode surface

in hydrogen DC arc-discharge", Carbon 40 (2002) pp.2423-2428.

14. Kazuyoshi Tanaka, Satoru Nishio, Yukihito Matsuura and Tokio Yamabe, "Preparation of Organic Semiconductive Thin Film by Plasma-Polymerization of Aromatic Compounds and Their Derivatives", Synthetic Metals, 55-57 (1993) pp.896-901.

15. M. Homann, K. Schmidt, T. Fritz, T. Hasche, V.M. Agranovich, K. Leo, "The lowest energy Frenkel and charge-transfer excitons in quasi-one-dimensional structures: application to MePTCDI and PTCDA crystals", Chemical Physics 258 (2000) pp.73-96.

16. Ricardo Mercadante, Milan Trsic, Jim Duff, Ricardo Aroca, "Molecular orbital calculations of perylenetetracarboxylic monoimide and bisimide. Alkyl derivatives and heteroatom analogs", Journal of Molecular Structure (Theochem) 394 (1997) pp.215-226.

17. F. Bogar, W. Forner, E. Kapuy, J. Ladik, "Correlation-corrected energy bands of polymers with large unit cell: poly(para-phenylene) and poly(peri-naphthalene)", Journal of Molecular Structure (Theochem) 391 (1997) pp.193-199.

18. Martin L. Kaplan, Paul H. Schmidt, Cheng-Hsuan Chen, and Walter M. Walsh, Jr., "Carbon films with relatively high conductivity", Appl. Phys. Lett. 15 May 1980, 38(10), pp.867-869.

19. J.L. Bredas, "Theoretical study of the electronic properties and crystal structure of poly(perinaphthalene): On the origin of high observed conductivities", J. Chem. Phys. 83 (3), 1 August 1985, pp.1316-1322.

20. N. Tyutyulkov, A. Tadjer and I. Mintcheva, "Band structure of poly(perinaphtalene)", Synthetic Metals, 38 (1990) pp.313-317.

21. P.M. Viruela, R. Viruela, and E. Ortf, "Influence of nitrogen substitution on the electronic band structure of poly(peri-naphthalene)", Synthetic Metals 69 (1995) pp.705-706.

22. Hiroaki Kamo, Masako Yudasaka, Susumu Kurita, Takeo Matsui, Rie Kikuchi, Yoshimasa Ohki, Susumu Yoshimura, "Formation of poly-peri-naphthalene thin film by chemical vapor deposition", Synthetic Metals 68 (1994) pp.61-63.

23. S. Nishio, A. Matsuzaki and H. Sato, "Preparation of low-dimensional conducting polymer films by UV light-induced deposition with excimer laser beams", Synthetic Metals 84(1997) pp.367-368.

24. S. Zyoshimura, M. Murakami, H. Yasujima and S. Mizogami, "New polyconjugated systems for intrinsically conductive polymers", Synthetic Metals, 18 (1987) pp.473-478.

25. Harris, Peter J. F. (Peter John Frederich), "Carbon nanotubes and related structures: new materials for the 21st century", Cambridge, UK ; New York : Cambridge University Press, 1999. ISBN: 0521554462 (hc).

26. http://www.lesker.com/newweb/menu_techinfo.cfm?CFID=235616&CFTOKEN=38557132.

27. "Vacuum Technology: Its Foundations, Formulae and Tables", LEYBOLD INC. October 1987.

28. Craig A. Taylor, Wilson K.S. Chiu, "Characterization of CVD carbon films for hermetic optical fiber coatings", Surface and Coatings Technology 168 (2003) pp.1-11.

29. V. Meenakshi and S. V. Subramanyam, "Medium-range order in pyrolyzed carbon films: Structural evidence related to metal–insulator transition", J. Appl. Phys., Vol. 92, No. 3, 1 August 2002, pp.1372-1379.

30. V. Meenakshi and S.V.Subramanyam, "Medium-range order in pyrolyzed carbon films: Structural evidence related to metal-insulator transition", J.Appl. Phys., Vol. 92, No. 3, 1 August 2002, pp.1372-1379.

31. http://www.aquila.infn.it/infm/labinfm/infm_oth/attr/.

32. S.R. Forrest, M.L. Kaplan, P.H. Schmidt, T. Venkatesan, and A.J. Lovinger, "Large conductivity changes in ion beam irradiated organic thin films", Appl. Plys. Lett. 41 (8), 15 October 1982, pp.708-710.

33. N.S. Murthy, S.O. Dantas, Z. Iqbal, R.J. Baughman, "X-ray diffraction evidence for the formation of a discotic phase during graphitization", Carbon 39 (2001) pp.809-813.

34. http://www.mos.org/sln/SEM/.

35. Mukul Kumar, Yoshinori Ando, "Single-wall and multi-wall carbon nanotubes from camphor—a botanical hydrocarbon", Diamond and Related Materials (2003), ARTICLE IN PRESS.

36. N.S. Murthy, S.O. Dantas, Z. Iqbal, R.J. Baughman, "X-ray diffraction evidence

for the formation of a discotic phase during graphitization", Carbon 39 (2001) pp.809-813.

37. M. Yudasaka, Y. Tasaka, M. Tanaka, H. Kamo, Y. Ohki, S. Usami, and S. Yoshimura, "Polyperinaphthalene film formation by pulsed laser deposition with a target of perylenetetracarboxylic dianhydride", Appl. Phys. Lett. 64(24), 13 June 1994, pp.3237-3239.

38. "Air Quality Guidelines - Second Edition WHO Regional Office for Europe", Copenhagen, Denmark, 2000.

39. Paul H. Schnidt, David C. Joy, Martin L. Kaplan, and William L. Feldmann, "Electron beam pattern generation in thin film organic dianhydrides", Appl. Phys. Lett. 40(1), 1 January 1982, pp.93-95.

40. Satoru Nishio, Kazuyuki Tamura, Yukari Tsujine, Tomoko Fudao, Masayoshi Nakano, Akiyoshi Matsuzaki, Hiroyasu Sato, "Remarkable enhancement on elimination reaction of side groups in excimer laser ablation of mixture targets of perylene derivatives with metal powder", Applied Surface Science 197-198(2002) pp.764-767.

41. Charanjeet Singh Paur, "Crystallographic structure and mechanical properties of tantalum coatings on steel deposited by DC magnetron sputtering", A thesis of New Jersey Institute of Technology, Interdisciplinary Program in Materials and Engineering, August 2002.

42. http://www.trdspecialties.com/default.asp.

43. Satoru Nishio, Ryoko Mase, Tetsuya Oba, Akiyoshi Matsuzaki, Hiroyasu Sato, "Preparation of amorphous organic semiconductor thin films with polyperinaphthalene structure on temperature-controlled substrates by excimer laser ablation of 3,4,9,10-perylenetetracarboxylic dianhydride", Applied Surface Science 127-129 (1998) pp.589-594.

44. Garratt, Peter J. (Peter Joseph), "Aromaticity", New York: Wiley, c1986, ISBN: 0471807036.

45. http://ptcl.chem.ox.ac.uk/MSDS/.

46. K.Kamiya, T. Noda, M. Idc and J. Tanaka, "Characterization of carbon films prepared by pyrolysis of perylenetetracarboxylic dianhydride", Synthetic Metals 71 (1995) pp.1765-1766.

47. Zhong-Sheng Wang, Chun-Hui Huanga, Fu-You Li, Shi-Fu Weng, Shu-Ming

Yang, "Photosensitization of nanocrystalline TiO2 electrodes with II B group metal-ion-bridged self-assembled films of 3,4,9,10-perylene tetracarboxylic acid", Journal of Photochemistry and Photobiology A: Chemistry 140 (2001) pp.255–262.

48. http://chrom.tutms.tut.ac.jp/JINNO/DATABASE/00database.html.